Summary on

Noise and Signal-to-Noise in Photodetector Systems

by David Kleinfeld

(Sept. 7, 1979)

PREFACE

This report summarizes research done on sensitivity considerations in photodetector systems. It addresses itself to questions concerning signal-to-noise ratios in photodetectors and amplifiers and optimum sample optical densities. It does not address the topic of optimal signal filtration as a way of increasing sensitivity.

All of the results described here have been discussed in a series of six two-hour group seminars presented during the winter 1978 school quarter. Some of the topics addressed in the report are the result of questions raised during these seminars. In addition, there was a seminar on the physics of PIN photodiodes, and a workshop held on the fundamentals of operational amplifier circuits.

The outcome of this research has helped with the design and implementation of a new photodetector system for monitoring the optical signature of light-induced kinetic changes of interest in the microsecond to millisecond time regime. This system has improved the signal-to-noise ratio of the data collected considerably over that obtained with the previous system. The research has also led to an understanding of the optimal optical density to use in the kinetic experiments.

TABLE OF CONTENTS

0. INTRODUCTION

This report examines the sources of noise in photodetection systems and the optimization of signal to noise ratios (S/N)[1] for various experimental configurations. Photodetector systems are typically employed in our laboratory for the measurement of transient optical changes in biochemical systems. We focus on photodetectors sensitive in the visible and near IR optical regions.

A photodetection system can be represented schematically as shown in Figure 0.1.

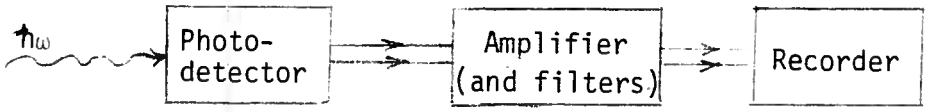

Fig. 0.1

The detector and the amplifier will individually generate noise and there may be cooperative effects. The photodetector can be either a photomultiplier tube or a PIN photodiode. Other types of semiconductor photodetectors exist (such as PN photodiodes, CdS photocells), but are generally not of interest for our laboratory due to poor linearity, optical bandwidth and/or transient response time.

There are three topics I will discuss concerning photodetector noise. The first is the question of the minimum detectable light level due to intrinsic detector noise in the dark. The second concerns the noise levels at light intensities well above the level of minimum detectability and the limiting signal-to-noise ratios S/N in this case. The last concerns the S/N for the case of measuring small changes in light levels over a large background level. In this regard, I also discuss the problem of optimizing the samples' optical density

---

[1] I will express the S/N ratio as the ratio of light-induced signal currents to noise currents, rather than the usual ratio of powers. This is because one typically measures currents, not powers, in spectroscopic experiments.

for the best S/N. I also discuss noise in operational amplifiers pertinent to their use as current to voltage converters and their interation with different detectors. Finally, I will make conclusing remarks on the merit of different photodetector systems, and give some practical examples.

I. Minimum Optical Detectability

Photomultiplier Tubes.

When a photomultiplier tube is biased by a high voltage supply to its operating point, there will always be a small anode current in the dark due to thermeonic emission at the cathode and dynodes. This dark current, I_{AD}, causes a shot noise given by

$$I_n = \sqrt{2eI_{AD}G\ \Delta\nu} \tag{1.1}$$

where e is the electronic charge, G is the current amplification of the photomultiplier tube, and $\Delta\nu$ is the bandwidth in Hertz. The standard definition of minimum detectability specifies a light generated current equal to the shot noise current. This corresponds to a S/N of $1/\sqrt{2}$. The optical power required to generate this current is commonly called the noise effective power (NEP), or the equivalent noise input (ENI). This value, in units of $W/\sqrt{Hz}$, is given by[2]

$$NEP = \frac{\sqrt{2eI_{AD}G\ \Delta\nu}}{\mathcal{R}(\lambda)G} = \frac{1}{\mathcal{R}(\lambda)}\sqrt{\frac{2eI_{AD}\ \Delta\nu}{G}} \tag{1.2}$$

---

[2]One expects that the NEP should be independent of gain. Since photodetection takes place at the cathode, it is actually more fundamental to talk of an effective cathode dark current, I_{CD}, where $I_{AD} = GI_{CD}$. One then finds that

$$NEP = \frac{\sqrt{2eI_{CD}\ \Delta\nu}}{\mathcal{R}(\lambda)}.$$

where $\mathcal{R}(\lambda)$ is the cathode responsivity[3] in units of A/W. $\mathcal{R}(\lambda)$ is wavelength dependent in a way that makes the NEP relatively constant over some range of wavelengths and fall off very rapidly outside this range. Fig. 1.1 illustrates $\mathcal{R}(\lambda)$ versus λ for various photomultiplier tubes.

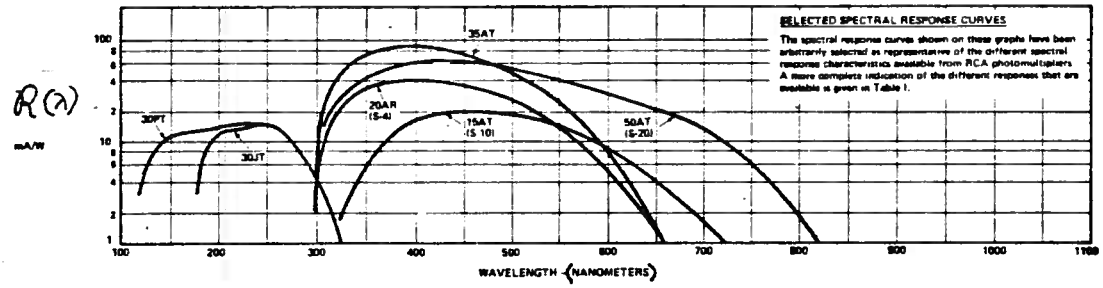

Typical Ultraviolet and Visible Spectral Response Characteristics

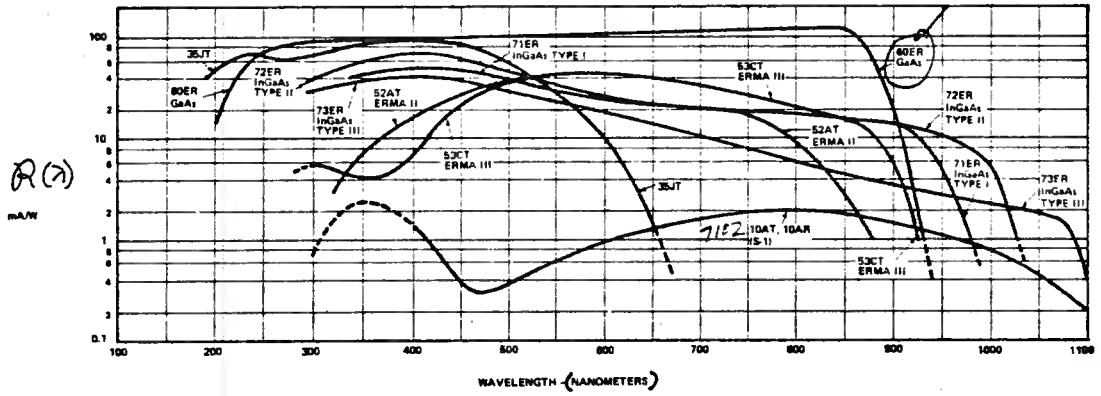

Typical "Broadband" Spectral Response Characteristics

Figure 1.1

Typical values for phototubes sensitive at 865 nm (such as the Hamamatsu 955, 636, or 666, or RCA 81034) give NEP's around .8 - 1.2 x 10^{-15} W/$\sqrt{\text{Hz}}$ at room temperature. These devices have active areas of $\sim$ 1 cm^2. For example, when monitoring at 865 nm, this corresponds to $\sim$ 4500 photons/sec into a 1-Hz bandwidth. The most sensitive phototubes available are the Varian VPM 167 series, which have NEP's as low as 1 x 10^{-18} W/$\sqrt{\text{Hz}}$ at 865 nm and room temperature. These detectors, however, are extremely costly, $3,000-$6,000, compared with a few

[3]The cathode responsivity, $\mathcal{R}(\lambda)$, is directly related to the cathode quantum efficiency, Q.E. by

$$\mathcal{R}(\lambda) = \frac{\lambda(\text{in nm})}{1240} \times \text{Q.E.} \quad .$$

1240 nm is the wavelength at which photons have an energy of 1 eV.

hundred dollars for the previously mentioned photomultiplier tubes. It is very important to note that the anode dark current in all photomultiplier tubes falls off exponentially with inverse temperature until it reaches some minimum valve, generally a factor of 10^{-5}-10^{-7} below the room temperature valve.[4,5] Thus, one can gain a factor of $\sim 10^{-3}$ in the NEP by cooling the photomultiplier tube, giving NEP's as low as 1×10^{-21} W/$\sqrt{\text{Hz}}$ at 865 nm for the Varian photomultiplier tubes ($\sim$ 1 photon/5 minutes in 1 Hz B.W.).

Photodiodes

A photodiode, unbiased and in the dark, exhibits thermal noise due to the finite resistance of the depletion layer. This noise current, I_N, sometimes called the junction leakage current, is given by

$$I_N = \sqrt{\frac{4KT\ \Delta\nu}{R_p(0)}} \tag{1.3}$$

where $R_p(0)$ is the dynamic resistance of the diode at zero bias. This relation was confirmed experimentally for the United Detector Technology (UDT) models 6D and 10D photodiodes. For PIN photodiodes, $R_p(0)$ scales with the size of the photodiode active area, being $\sim$ 15MΩ/cm for the popular UDT "D" series.

---

[4]This decrease is due to the drop in thermeonic emission from the cathode. The thermeonic current is proportional to $T^2\exp\{-E_{W.F.}/kT\}$ where $E_{W.F.}$ is the work function of the photocathode, typically 1.0 - 1.2 eV for photomultiplier tubes sensitive in the near I.R. The NEP is thus proportional to $\exp\{-E_{W.F.}/2kT\}$.

[5]The leveling off of the anode dark current as $T \to 0$ may be due to electronic emission induced by background radiation. However, this effect was not carefully researched by the author.

The NEP is expressed as:

$$NEP = \frac{\sqrt{\frac{4KT\ \Delta\nu}{R_p(0)}}}{\mathcal{R}(\lambda)} \qquad (1.4)$$

where $\mathcal{R}(\lambda)$ is the responsitivity in Amps current/Watts light at zero bias. For a detector with a 1-cm^2 active area, a typical value of NEP is 10^{-12} W/$\sqrt{Hz}$. The UDT 20 detectors, with .004 cm^2 active area, have the lowest available NEP's at 6×10^{-15} W/$\sqrt{Hz}$. The NEP is a strong function of temperature through the temperature dependence of $R_p(0)$. $R_p(0)$ is dominated by the P-I and I-N junction resistance, which is proportional to $\exp\{E_g/kT\}$, where E_g is the gap energy. This relation was tested experimentally for the UDT 10D photodiode. The results are shown in Figure 1.2, which plots $R_p(0)$ vs. 1/T. Note that the slope of the line predicts E_g = 1.2 eV, close to the known value of 1.1 eV for silicon. Thus, the NEP is proportional to $\exp(-E_g/2kT)$, a temperature dependence very similar to that for the NEP in photomultiplier tubes, since $E_{W.F.} \simeq E_g$.

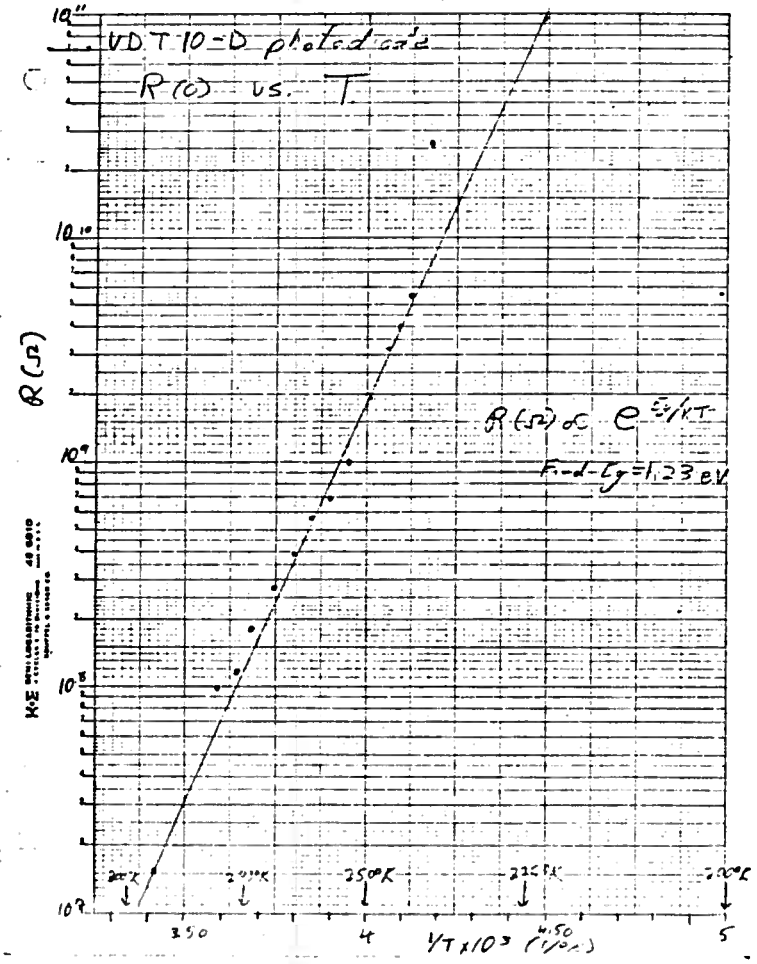

Figure 1.2

The responsivity of the photodiode is expected to increase at 0.1% per volt reverse bias.[6] However, we also increase the total noise due to the addition of a reverse bias current shot noise. For this case,[7] the NEP becomes

$$\text{NEP(bias} \neq 0) = \frac{\sqrt{\frac{4KT\ \Delta\nu}{R_p(0)} + 2eI_B\ \Delta\nu}}{\mathcal{R}(\lambda, V_{bias})} \qquad (1.5)$$

where I_B is the bias current.[8] For the UDT 6D diode, I measured an $\sim$ 2.5% increase in the responsivity with a 22V reverse bias (I_D = 23 mA). However,

---

[6]From the "Silicon Photodetector Design Manual," UDT Company

[7]The noise in a diode is due to carrier fluctuations through the depletion layer. The total current through this layer is given by the Schottky equation,

$$I = I_s(e^{eV/kT} - 1),$$

where I_s is the reverse bias saturation current, and V is the bias potential. The first term in this expression is due to minority carriers, the second majority carriers. Each component is statistically independent of the other and will yield full shot noise. Thus:

$$I_N = 2e\ I_s e^{eV/kT} + 2e\ I_s$$

$$" = 2e\ (I_s + I_B) + 2e\ I_s$$

$$" = \frac{4kT}{R_p(0)} + 2e\ I_B$$

where $1/R_p(0) = \left.\frac{dI}{dV}\right|_{V=0}$ and I_B is the applied bias current. Note that this result gives the thermodynamic noise at zero bias. This type of derivation is similar to one used by Aldert Van Der Ziel in "Proceedings of the IEEE," Vol. 58, No. 8, 1970.

[8]$I_B \leq I_s$ under reverse bias conditions. Equality holds when $|V_{bias}| >> \frac{kT}{e}$.

the shot noise is now $\sim$ 7 times the thermal noise, so the NEP has actually increased by a factor of $\sim$ 2.5. Similar results were found with the UDT 10D diode. Note also that below $\sim 10^3$ Hz, there can be "1/f" noise present due to the bias current, raising the NEP even more at low frequencies. Such excess noise was found for the UDT 6D and 10D diodes.[9] Thus, the lowest NEP for PIN photodiodes is achieved when the photodiode is operated in the unbiased mode.

Concluding Remarks

In terms of absolute sensitivity, phototubes are clearly preferable. At room temperature, the typical phototubes are about 3 orders of magnitude more sensitive than the photodiodes for equal photosensitive areas. This difference is 2-3 orders of magnitude greater for the better phototubes. Both photodiodes and photomultiplier tubes show roughly the same improvement of the NEP with lowered temperature. Photodiode NEP can be improved by using devices with smaller active areas, there being an $\sim 2\frac{1}{2}$ order of magnitude improvement in going from a 1 cm^2 device to a .004 cm^2 device. Practical considerations will dictate whether the light source of interest can be focused down to such a small area.

If one is trying to detect light signals where the low NEP photodiodes are adequately sensitive, practical considerations will dictate the choice of photodiode or photomultiplier tube. The differences in active area is one consideration. In terms of total volume, photodiodes are small compared to photomultiplier tubes, as are all semiconductor devices compared to their vacuum tube antecedents. Photomultiplier tubes require external power supplies capable of supplying 1,000-2,000 volts D.C. and may require external resistance networks for biasing the dynode stages. This adds to the cost and complexity of their use. Photodiodes are about a factor of 10 less in cost than photomultiplier

[9]This point will be discussed in detail in part II.

tubes (typically \$10-\$50) and, for low-light detection, require no bias supply. Photomultiplier tubes have a built-in current gain typically in the range of 10^4-10^6, while photodiodes supply no such gain and thus must be coupled to sensitive preamplifiers. As discussed in Section V, this coupling may lead to decreased S/N.

II. Photodetector S/N When Detecting Above the NEP Limit.

Photomultiplier Tubes.

Photomultiplier tubes will exhibit full shot noise when generating a light-induced current. The total shot noise is

$$I_N = \sqrt{(2eGI_{AD} + 2eGI_{AL})\,\Delta\nu} \tag{2.1}$$

where I_{AL} is the light-induced anode current with

$$I_{AL} = P\,\mathcal{R}(\lambda)\,G$$

where P is the optical power in Watts. The light-induced shot noise contribution is just a manifestation of photon statistics. At powers greater than the NEP, $I_{AL} >> I_{AD}$ and the S/N ratio can be approximated as:

$$S/N \approx \frac{I_{AL}}{\sqrt{2eGI_{AL}\,\Delta\nu}}$$

$$" \approx \sqrt{\frac{P\mathcal{R}(\lambda)}{2e\Delta\nu}} \tag{2.2}$$

Note that the S/N is independent of the current amplification gain, as it must be, and that it scales as the square root of the cathode responsitivity or quantum efficiency.

The forgoing analysis assumed that there are no additional noise contributions from the photomultiplier tube dynode structure. Thus, Eq. (2.2) strictly

applies to the S/N at the photomultiplier tube cathode. Because of the finite gain of each dynode stage, fluctuations are added to the electron current as it is amplified. To calculate this effect, we note that if n electrons are incident on a dynode stage with gain g, the number of emitted electrons is $gn \pm \sqrt{gn}$. The next dynode stage, also with gain g, will emit $g^2n \pm g\sqrt{gn} \pm \sqrt{g^2n \pm g\sqrt{gn}}$ or $g^2n \pm \sqrt{(g^3 + g^2)n}$. After K dynode stages, each of gain g (this assumes a uniform dynode chain), there will be

$$g^K n \pm \sqrt{(g^{2K} + \ldots + g^K)n} \quad \text{or} \quad g^K n \pm g^K \sqrt{\frac{g-g^{-K}}{g-1}\, n} \quad \text{electrons.}$$

The random term is commonly called the partition noise. Thus, the signal-to-noise is degraded by a factor $\sqrt{\frac{g-1}{g-g^{-K}}}$. g is typically between 4 and 7 and if a few dynode stages are employed we can drop the g^{-K} term. Thus

$$\left.\frac{S}{N}\right|_{\substack{\text{PMT}\\ \text{Anode}}} \approx \sqrt{\frac{g-1}{g}}\ \sqrt{\frac{P\mathcal{R}(\lambda)}{2e\Delta\nu}} \quad . \tag{2.3}$$

For example, for g = 5, the S/N decreases by 11% between the cathode and the anode. The form of the partition noise shows that, in cases where the overall gain of a photomultiplier tube is to be lowered, it is best to reduce the number of dynode stages employed, keeping the gain per stage constant, rather than reduce the gain at each stage.

Another source of noise is due to fluctuations in the photomultiplier high voltage supply, which will cause fluctuations in the photomultiplier tube current gain and hence the output current. The light-induced anode current is related to the light-induced cathode current, I_{CL}, by

$$I_{AL} = GI_{CL} = g^n\ I_{CL}$$

where n is the number of dynode stages. g is related to the dynode voltage v

[where v = V/(n+1), V the voltage drop across the entire tube] by

$$g = kv^{\beta}$$

where k is a constant and β is determined by the material and structure of the dynode and usually has a value of $0.7 \sim 0.8$.[10] Thus

$$I_{AL} = kv^{\beta n} I_{CL}$$

and

$$\frac{\delta I_{AL}}{I_{AL}} = \beta n \frac{\delta V}{V} = \beta n \frac{\delta V}{V} \qquad (2.4)$$

where δ represents a variation. This constitutes an effective noise current of

$$I_n = \beta n I_{AL} \frac{\delta V}{V} \quad . \qquad (2.5)$$

δV will contain components due to 60 Hz ripple (typical $\delta V = .3 - 3 \times 10^{-3}$ V) fluctuation is line voltages (typical $\delta V = 1 - 2 \times 10^{-5}$ V times percent change in line voltage $\approx 10^{-4}$ times change in line voltage), long term drift (typical $\delta V = 10^{-4}$ V $\approx$ 100 mV over 8 hours), temperature variations ($\delta V \approx 5 \times 10^{-5}$ V/°C $\approx$ 50 mV/°C) and poor or loose connections. Note that this noise is fairly colored. To estimate the stability one needs in a high voltage power supply, I_n in Eq. (2.5) should be compared with the shot noise from the photomultiplier tube under typical experimental conditions.

Intrinsic "1/f" noise is not considered a problem in properly used photomultiplier tubes.[11] This topic was not investigated experimentally, except for a qualitative measurement of excess noise in the Hammamatsu R955 photomultiplier tubes. At frequencies down to 1 Hz, no excess noise was noted.

---

[10]Hammamatsu Photomultiplier Tube Catalog, page 5, February 1979.

[11]Conversation with RCA technical service department.

Other noise sources associated with but not intrinsic to photomultiplier tubes are microphonic noise and noise, possibly 1/f, due to loose, dirty, or damp connections in the photomultiplier bias circuit. Leakage currents due to dampness or poor photomultiplier tube base construction can be a particular problem. Some photomultiplier tubes, such as the Varian VPM-164 series, have built-in bias circuits and vacuum sealed.

Photodiodes

A photodiode will exhibit, at the minimum, full shot noise due to the light-induced current. When operated in the unbiased mode, the S/N is

$$\frac{S}{N} = \frac{I_L}{\sqrt{\left[\frac{4kT}{R_p(0)} + 2eI_L\right]\Delta\nu}} \tag{2.6}$$

where $I_L = \mathcal{R}(\lambda)P$. $\mathcal{R}(\lambda)$ is the diode responsitivity. At light levels greater than the NEP, this becomes

$$\left.\frac{S}{N}\right|_{P>>NEP} = \sqrt{\frac{P\mathcal{R}(\lambda)}{2e\Delta\nu}} \tag{2.7}$$

which is identical with the case for the S/N at the photomultiplier tube cathode. Typical $\mathcal{R}(\lambda)$'s for photodiodes are 4 to 7 times larger than those for photomultiplier tubes over their sensitive regions, so we expect, on the basis of shot noise, a gain in S/N.

All semiconductor devices are believed to possess excess noise that varies roughly as 1/f. For silicon photodetectors, excess noise currents, I_{EX}, of the form

$$I_{EX}^2 = \frac{I_L^2}{f^\gamma} \quad \text{with } \gamma \text{ near } 1$$

have been reported.[12] To confirm and quantify this excess noise in three available photodiodes, as a function of light intensity and frequency. The experimental setup for this experiment is shown in Figure 2.1.

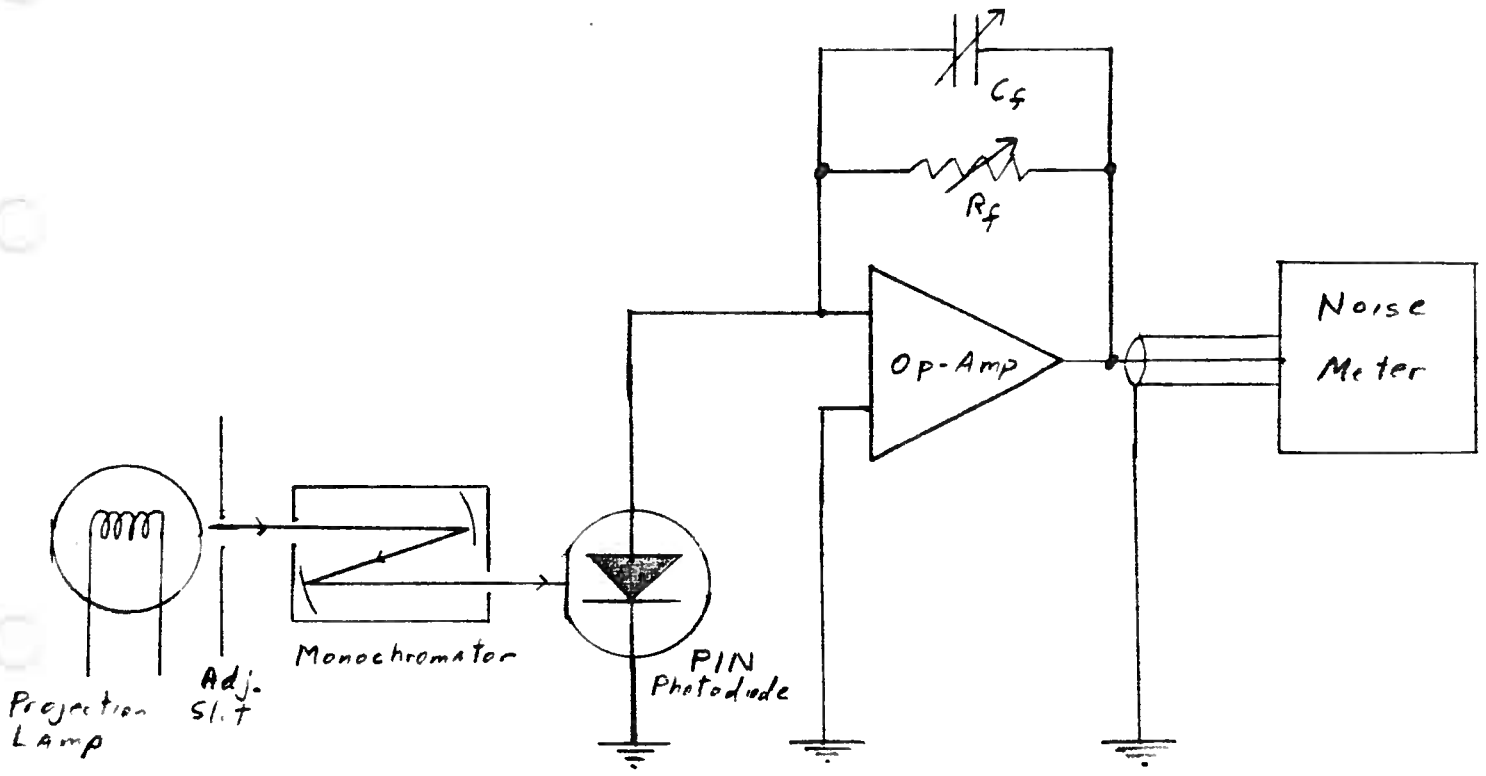

Figure 2.1

The measured noise consists of both diode noise and amplifier noise. Section IV covers the topic of noise in operational amplifier circuits in detail. The amplifier output consists of a light-induced voltage

$$V_L = Z_f \; I_L = Z_f \; \mathcal{R}(\lambda) \; P \qquad (2.8)$$

[12]Van Der Ziel.

and a noise voltage

$$E_N = \sqrt{\left[\left|1+\frac{Z_d}{Z_f}\right|^2 e_n + |Z_f|^2\left(i_n + \frac{4kT}{R_f} + \frac{4kT}{R_p(0)} + 2eI_L\right)\right]\Delta\nu + |Z_f|^2 I_{EX}^2} \quad (2.9)$$

where e_n is the op-amp voltage noise per $\sqrt{Hz}$, i_n is the op-amp current noise per $\sqrt{Hz}$, Z_f is the op-amp feedback impedance and Z_d the diode impedance. The photodiode is modeled as in Figure 2.2.

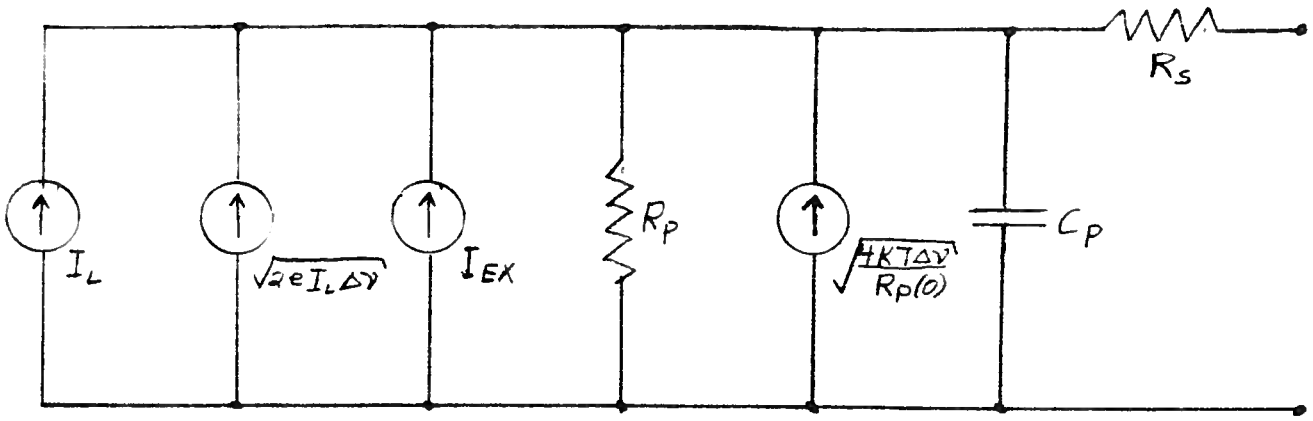

Figure 2.2

R_s, the diode series resistance is always orders of magnitude smaller than R_p and can be neglected. Then

$$Z_d = \frac{R_p}{1 + i\omega R_p C_p} .$$

For purposes of calculation we include cable capacity between the photodiode and the amplifier in C_p. The amplifier noise parameters were determined separately, as described in Section IV. Noise measurements were made with two different sets of equipment. For measurements on the UDT 10D photodiode, the signal was fed into a PAR HR-8 lock-in detector, employing a PAR Type D low noise preamplifier. The lock-in detector time constant was set to 100 msec and the input

bandpass filters set to 6 db/octave, providing a bandwidth of $\sim$ 1 Hz. The output from the lock-in detector was fed into a true RMS voltmeter of local design, employing an Analog Device 440K True RMS to DC converter. The true RMS voltmeter output was averaged for 200 seconds. The system was calibrated by measuring the Johnson noise from a 1 MΩ carbon film resistor. The system baseline was found by shortening the input to the lock-in detector preamplifier. Measurements on the HP 5082-4203 and UDT 6D photodiodes employed a General Radio Corporation model 1900 Wave Analyzer with a PAR model 113 preamplifier. The PAR was used in the AC-coupled mode with a bandwidth of .03 Hz to 300 KHz. The wave analyzer was set to a 10 Hz bandwidth and a 10V input saturation level. This system was also calibrated against the Johnson noise of a 1 MΩ resistor. The output of the wave analyzer was averaged for 200 seconds.

In all cases the photodiodes were illuminated with monochromatic light at 865 nm.

The excess noise was calculated by inverting Eq. (2.8) to solve for I_{EX}. I will give the results for the three photodiodes tested separately and compare the measurements at the end.

HP 5082-4203 Photodiode

This photodiode has an active area of 2×10^{-3} cm^2, a maximum responsivity $\mathcal{R}(\lambda = 770\ \text{nm}) = .5$A/W and a $\mathcal{R}(\lambda = 865) = .3$ A/W. The measured $R_p(0)$ is 9 GΩ giving a calculated NEP of 4×10^{-15} W/$\sqrt{\text{Hz}}$ versus a specified NEP of 5×10^{-14} W/$\sqrt{\text{Hz}}$. The unbiased junction capacitance is $\sim$ 3 pF.

Figures 2.3 and 2.4 are plots of excess photodiode noise current (I_{EX}) versus light induced current (I_L) at 100 Hz and 300 Hz, respectively. The circles are data points and the x's show the shot noise level at various light intensities for comparison purposes. At both frequencies we find that I_{EX} varies linearly with I_L. Figures 2.5 and 2.6 are plots of I_{EX} versus frequency at optical powers of 2.5×10^{-7} W and 8×10^{-7} W, respectively. In both cases, I_{EX} falls off as $1/f^{1-2}$ between $\sim$ 100 and 1000 Hz, and flattens off below $\sim$ 100 Hz. Importantly, I_{EX} falls to the shot noise level at $\sim$ 1000 Hz for both optical powers. The dotted lines in Figures 2.5 and 2.6 represent noise data taken as a continuous function of frequency with the Federal Scientific 10A Spectrum Analyzer. The magnitudes do not scale due to a systematic error, but the overall shape of the curve agrees with the previous data, and thus the curves are presented for illustrative purposes.

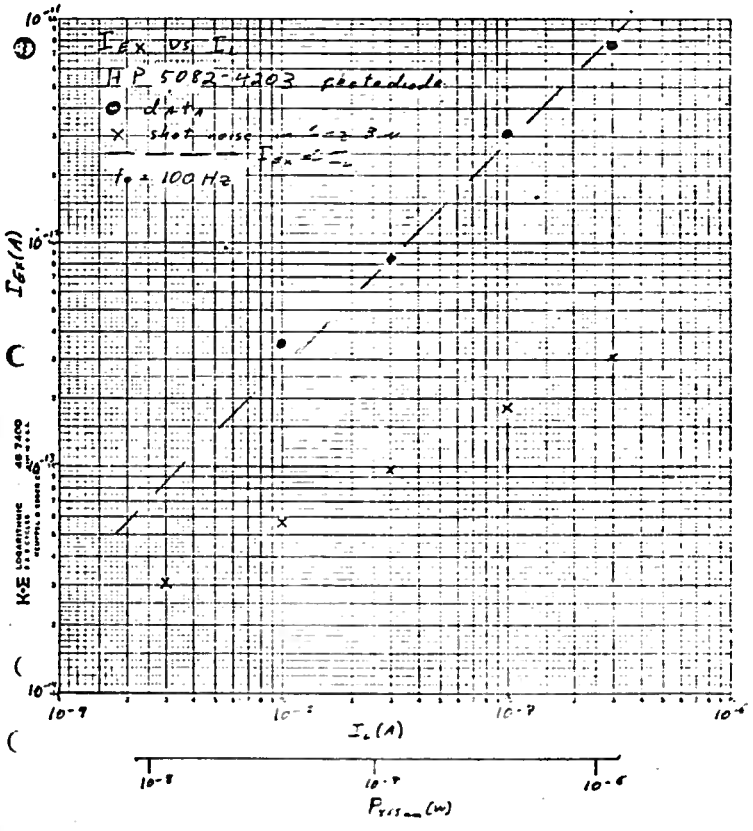

Figure 2.3

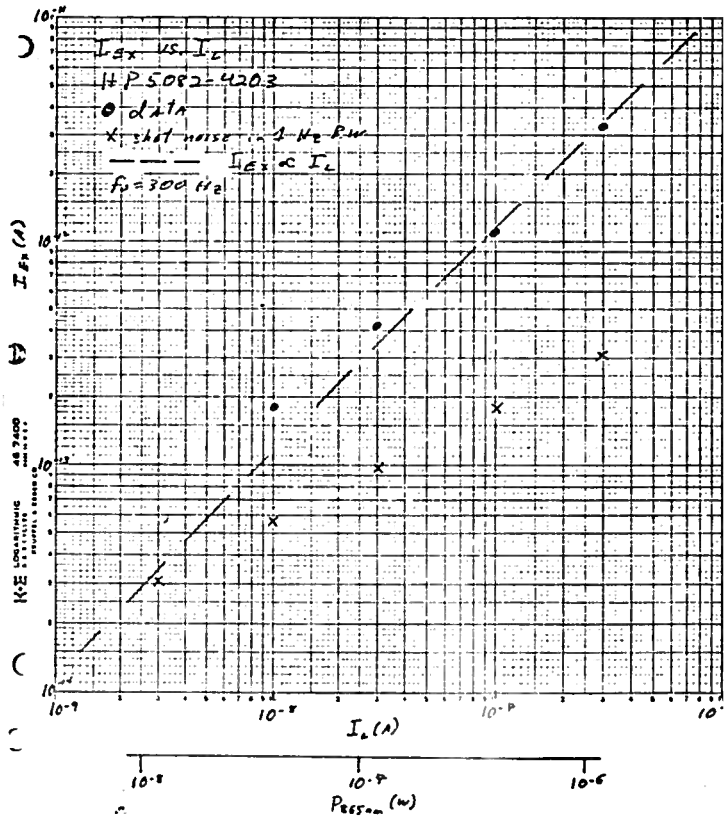

Figure 2.4

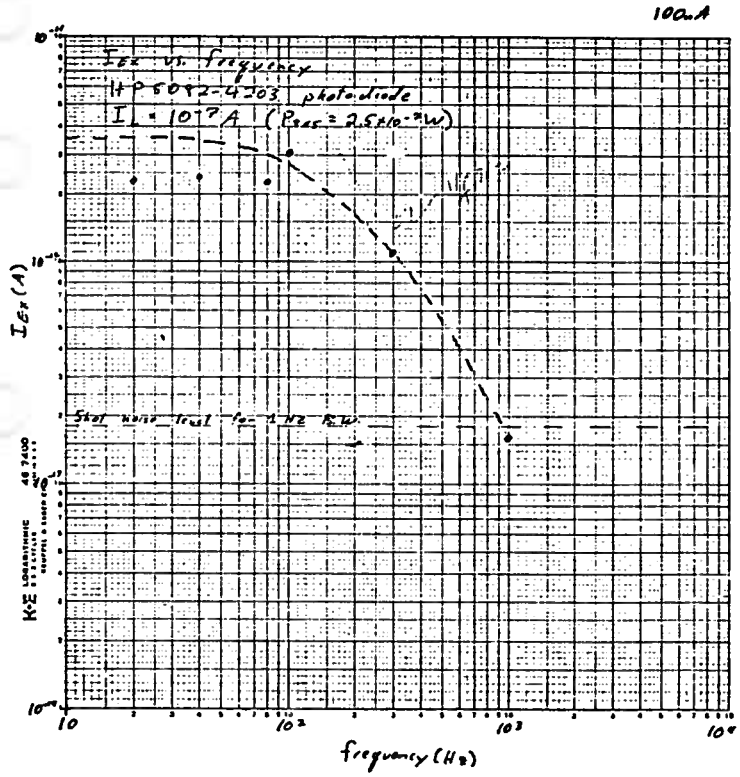

Figure 2.5

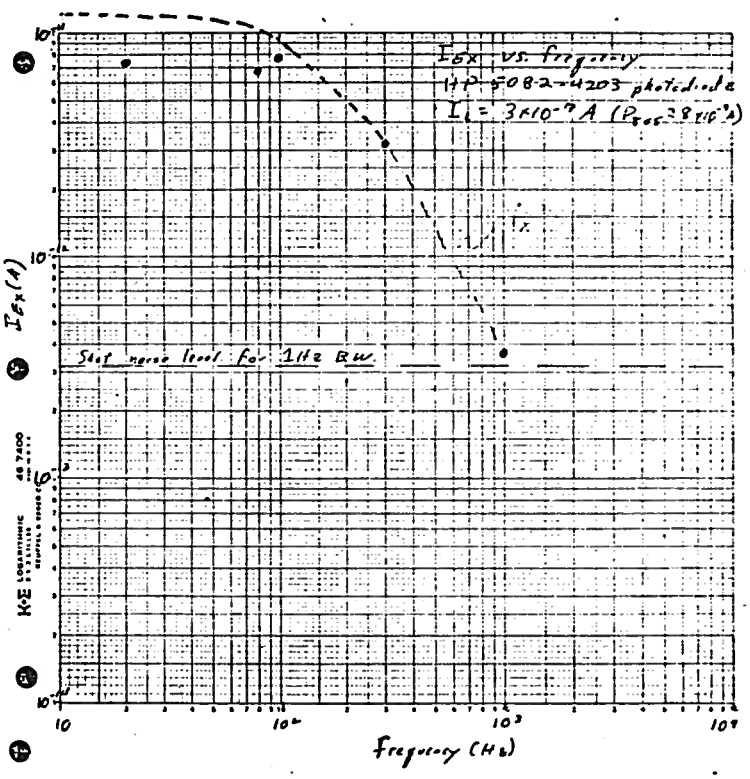

Figure 2.6

UDT 6D Photodiode

This photodiode has an active area of .203 cm^2 and maximum responsivity $\mathcal{R}(\lambda = 850\ nm) = .4$ A/W. The measured $R_p(0)$ is 90 MΩ, giving a calculated NEP of 4×10^{-13} W/$\sqrt{Hz}$ versus a specified NEP of 8×10^{-13} W/$\sqrt{Hz}$. The unbiased junction capacitance is ∿ 120 pF. The UDT 6D photodiodes received from the manufacturer exhibited a drifting bias current, and this may reflect itself in the noise properties of these diodes.

Figure 2.7 is a plot of I_{EX} versus I_L at a frequency of 100 Hz. As before, note that I_{EX} is linearly proportional to I_{EX}. Figures 2.8, 2.9, and 2.10 are plots of I_{EX} versus frequency for optical powers of 2.5×10^{-7} W, 8×10^{-7} W, and 2×10^{-6} W, respectively. The excess current noise rolls off as $1/f^{8-1}$ with frequency and, unlike the case of the HP5082-4203 and UDT 10D photodiodes, does

not flatten off at low frequencies. The excess current noise falls below the shot noise level at ∿ 400 Hz.

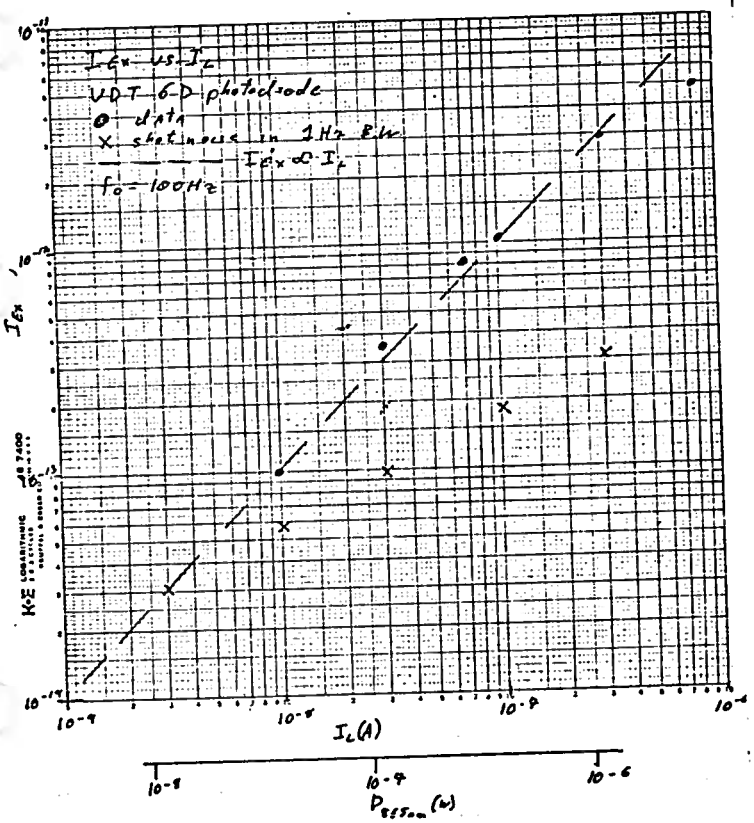

Figure 2.7

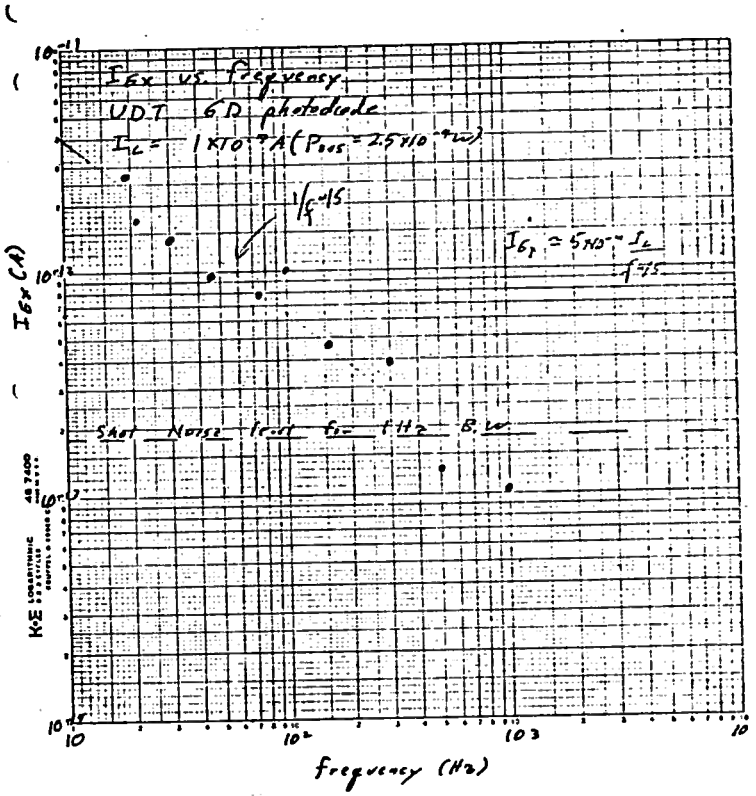

Figure 2.8

UDT 10D Photodiode

This photodiode has an active area of 1.00 cm^2 and a maximum responsivity $\mathcal{R}(\lambda = 850\ nm) = .4$ A/W. The measured $R_p(0)$ is 15 MΩ, giving a calculated NEP of 8×10^{-13} W/$\sqrt{Hz}$ versus a specified value of 10^{-12} W/$\sqrt{Hz}$. The unbiased junction capacitance is ∿ 650 pF.

Figures 2.11 and 2.12 are plots of I_{EX} versus I_L at 10 Hz and 100 Hz, respectively. Again, we see that I_{EX} is linearly proportional to I_L. Measurements of I_{EX} versus I_L were attempted at 1000 Hz. However, the excess noise level was too small to determine with any accuracy, except at $I_L = 3 \times 10^{-7}$ A

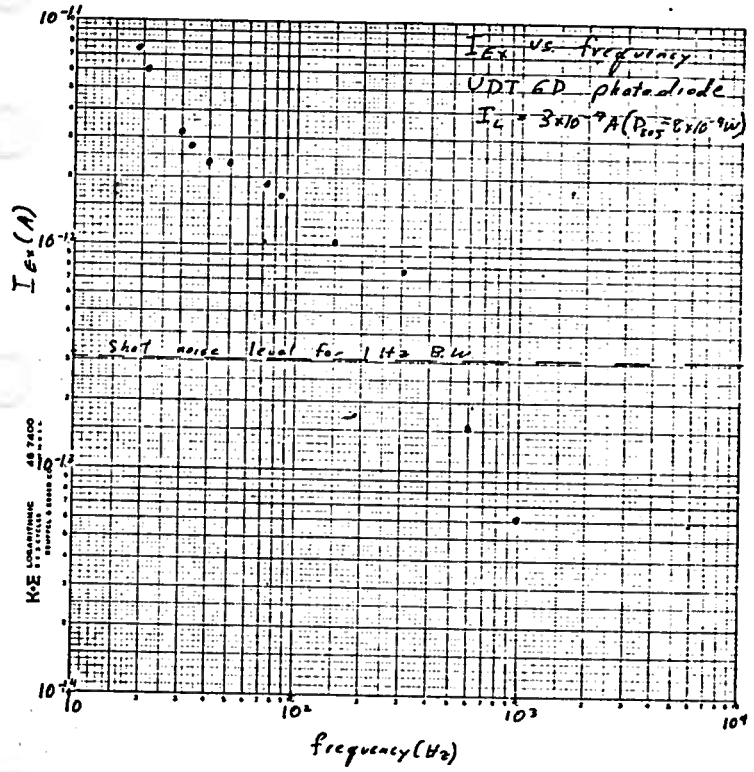

Figure 2.9

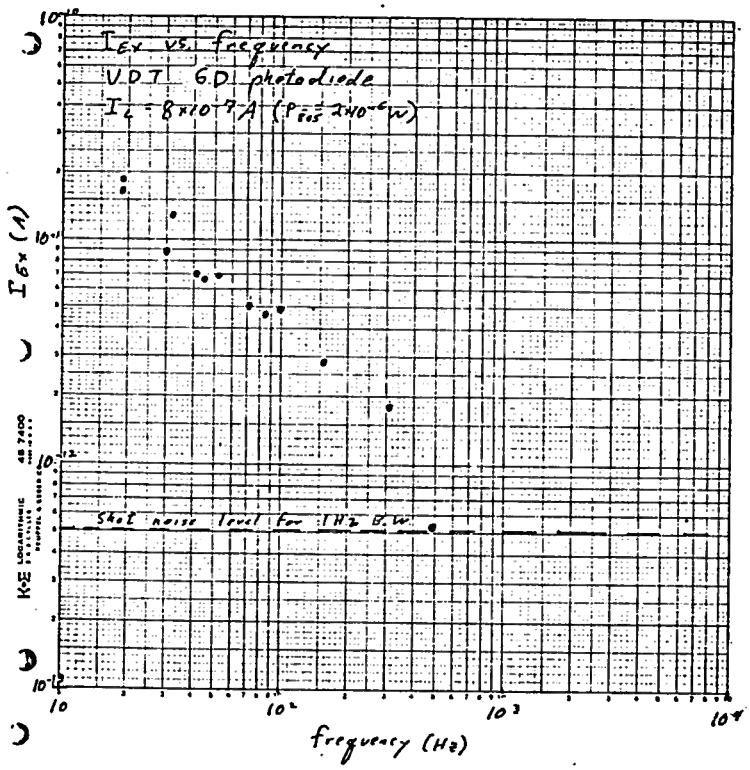

Figure 2.10

($P \approx 8 \times 10^{-7}$ W), where I found $I_{EX} \approx 3 \times 10^{-13}$ A in a 1 Hz bandwidth. Figure 2.13 is a plot of I_{EX} versus frequency for an optical power of 8×10^{-7} W ($I_L = 3 \times 10^{-7}$ A). Though there are only three data points, we again see a leveling off of I_{EX} at low frequencies and a fall to the shot noise level at 1 KHz. The low frequency leveling off of the noise was confirmed qualitatively using the Federal Scientific UQ-10 Spectrum Analyzer.

We see that for the photodiodes tested, the excess noise is given by

$$I_{EX}^2 = I_L^2 \quad \alpha(f) \tag{2.10}$$

where the function $\alpha(f)$ monotonically decreases with frequency in a nonsimple way. Above $\sim$ 1000 Hz, the excess noise is below the shot noise level, allowing us to neglect it for photodetector systems designed to operate above this fre-

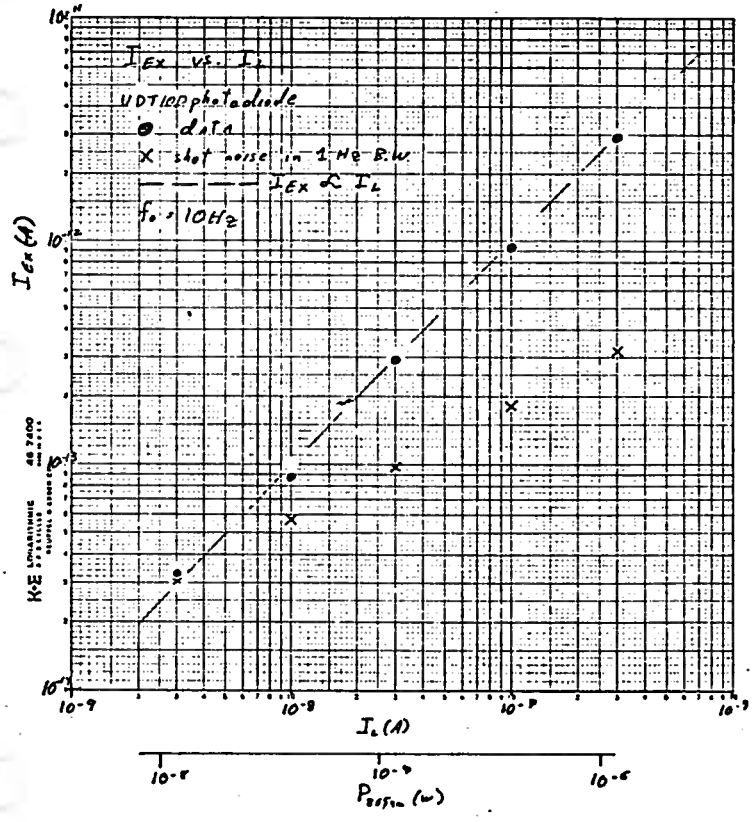

Figure 2.11

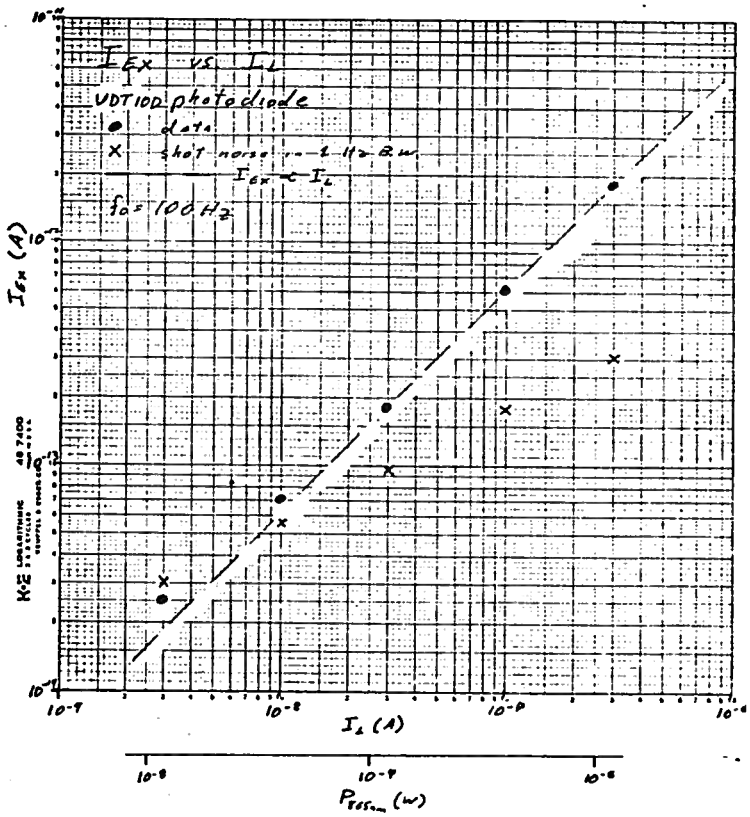

Figure 2.12

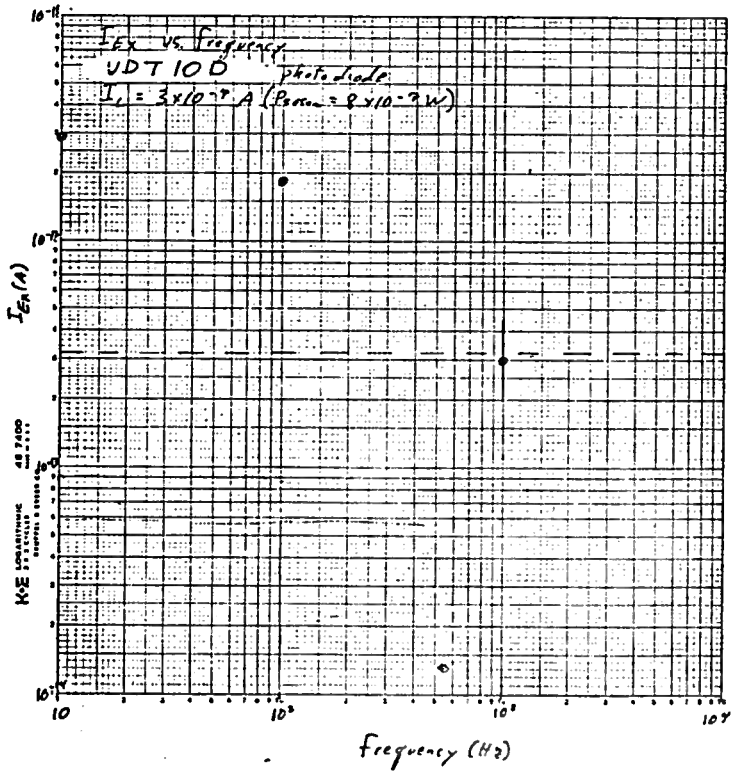

Figure 2.13

quency. Note that the excess noise increases as the diode surface area decreases. The form of Eq. (2.10) shows that in the limit of high optical power, $I_N \simeq \sqrt{\alpha(f)'}\ I_L$ and

$$S/N \approx \frac{1}{\sqrt{\alpha(f)'}} = \text{constant.}$$

Concluding Remarks

In comparing photomultiplier tubes and photodiodes, we have to weigh two competing factors. The responsivities of photodiodes are in general greater than those for photomultiplier tubes. Since $S/N \sim \sqrt{\mathcal{R}(\lambda)'}$, this fact favors photodiodes. Photodiodes, however, suffer from excess noise at frequencies below $\sim$ 1000 Hz, while photomultiplier tubes are free from this problem. The exact choice of device will depend on the frequency range and light intensity of interest and the weighing of these two factors. As a possible aid in circumventing the problem of excess low frequency diode noise when measuring a slowly varying signal (< 100 Hz), one could employ phase-sensitive detection. For example, the light beam eventually reaching the photodetector is chopped at 1000 Hz, and the output of the photodetector is passed through a lock-in amplifier set at the same frequency. The signal is now centered around 1000 Hz, away from the excess noise at the diode. This method, well known and commonly employed in scanning spectrophotometers, also diminished noise problems from microphonics, 60 Hz pick up, etc.

III. Photodetector S/N When Detecting Changes in Optical Signals and The Question of Optimal Sample Absorbance.

For many spectroscopic studies, we are interested in measuring a change in optical power, δP, over the background valve P, rather than an absolute power. In particular, this is the case for time resolved flash photolysis experiments. When the change in optical power, δP, reaching the detector is due to a change in absorbance, δA, of a sample, it is useful to express the S/N of the detector in terms of P_o, the optical power incident on the sample, A_o, the initial optical density of the sample, and δA. The relation among these variables is illustrated in Figure 3.1.

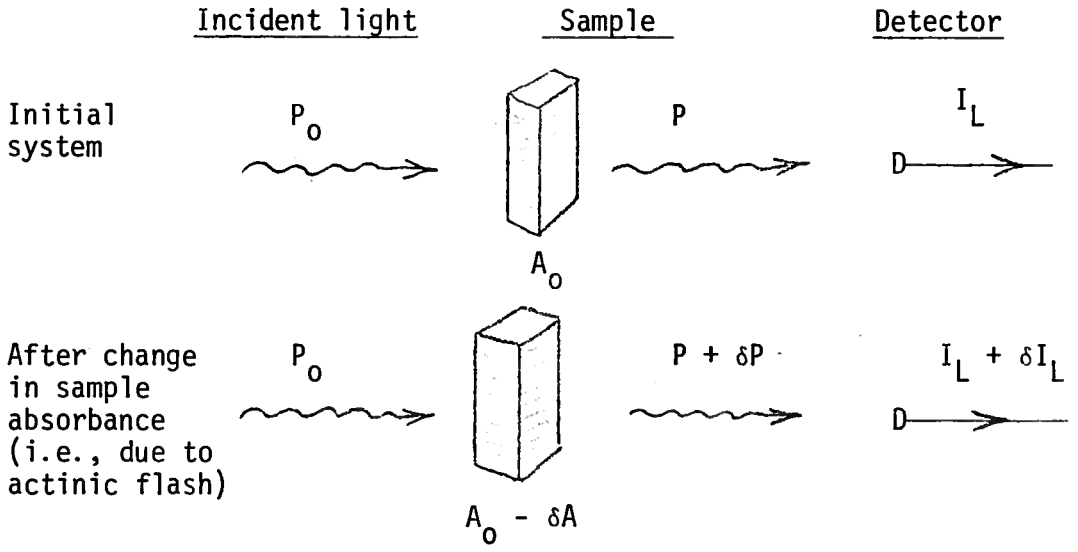

Figure 3.1

The exact relations between P_o, A_o, δA, P, and δP are

$$P = P_o e^{-2.3 A_o}$$

$$\frac{\delta P}{P} = e^{-2.3 \delta A} - 1 \qquad (3.1)$$

The factor 2.3 is the usual conversion from base 10 to base e. The signal current, δI_L, coming from the detector is

$$\delta I_L = \mathcal{R}\delta P$$

$$" = \mathcal{R}P_o\, e^{-2.3\, A_o}\,(e^{2.3\,\delta A} - 1)\,. \qquad (3.2)$$

The noise in the photodetector system can be expressed most generally as the incoherent sum of three terms. The first, I_{SH}, is the photodetector shot noise expressed as

$$I_{SH} = \sqrt{2e(I_L + \delta I_L)\,\Delta\nu}$$

$$" = \sqrt{2e\,\mathcal{R}P_o\, e^{-2.3(A_o-\delta A)}\,\Delta\nu}\,. \qquad (3.3)$$

The second represents the excess low frequency express current noise found in photodiodes, I_{EX}, which is proportional to I_L and falls off monotonically with increasing frequency. For our considerations, we write this noise as:

$$I_{EX} = \alpha(f)\ I_L$$

$$" = \alpha\,\mathcal{R}P_o\, e^{-2.3(A_o-\delta A)}\,. \qquad (3.4)$$

The third term, I_{IN}, is the incoherent sum of all noise sources independent of the signal. This includes the dark noise of the detector and noise introduced into the detection process by amplifiers. Thus, the total noise current, I_N, is expressed as:

$$I_N = \sqrt{2e\,\mathcal{R}P_o\, e^{-2.3(A_o-\delta A)}\,\Delta\nu + (\alpha\,\mathcal{R}P_o)^2\left(e^{-2.3(A_o-\delta A)}\right)^2 + I_{IN}^2}\,. \qquad (3.5)$$

Distinctly colored noise, such as power line (60 Hz) pick up or microphonics

is not considered, though it could easily be incorporated into Eq. (3.5) and would affect the $\delta S/N$ only in a specific time region. The $\delta S/N$ is:

$$\frac{\delta S}{N} = \frac{\delta I_L}{IN}$$

$$= \sqrt{\frac{\mathcal{R}P_o}{2e\Delta\nu}} \; \frac{e^{-2.3\,A_o}\left(e^{2.3\,\delta A} - 1\right)}{\sqrt{e^{-2.3(A_o-\delta A)} + \left(\frac{\alpha\mathcal{R}P_o}{I_{SH_o}}\right)^2 \left(e^{-2.3(A_o-\delta A)}\right)^2 + (I_{IN}/I_{SH_o})^2}} \qquad (3.6)$$

where $I_{SH_o}{}^2 = 2e\,\mathcal{R}P_o\,\Delta\nu$, the shot noise current when $P = P_o$ (i.e., $A = 0$).

Optimal Sample Absorbance

In flash photolysis experiments, the optical density of the sample decreases in response to an actinic flash. Clearly this decrease, δA, can be no larger than A_o. In general, we can write $\delta A = \mathcal{V} A_o$, where $\mathcal{V}$ is a time

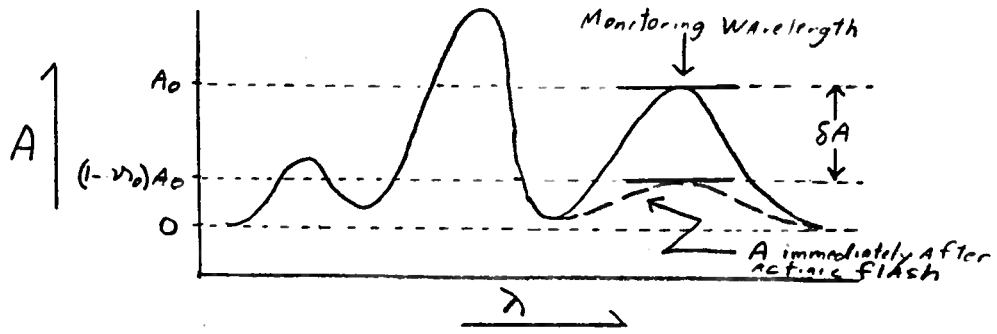

Figure 3.2a

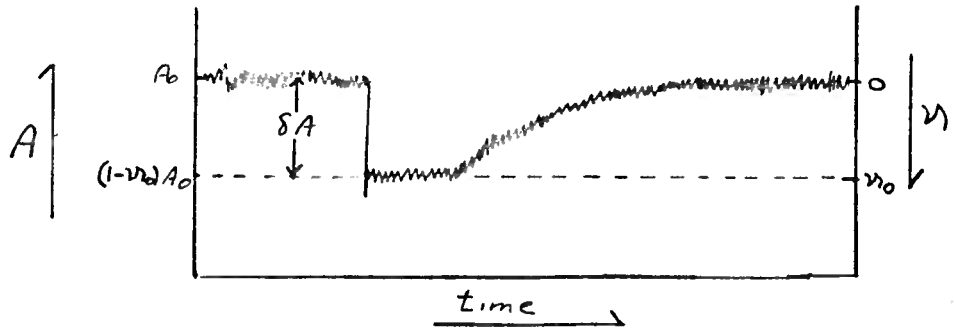

Figure 3.2b

dependent constant and $\eta \leq 1$.[13] This relation is illustrated in Figures 3.2a and 3.2b.

We can now find the value of A_o, as a function of η, that maximizes the $\delta S/N$. After some work we find the optimal A_o is given by solving the equation:

$$(1+\eta)-(1-\eta)\, e^{2.3\,\eta\, A_o} + 2\,(I_{EX}/I_{SH_o})\, e^{2.3\,A_o}\left[e^{-2.3\,A_o} - (1-\eta)\right] + 2\left(\frac{\alpha \mathcal{R} P_o}{I_{SH_o}}\right)\eta\, e^{-2.3(1-\eta)\,A_o} = 0 \quad . \tag{3.7}$$

This equation has no closed solution for A_o in terms of arbitrary η, α, and (I_{EX}/I_{SH_o}), but the limiting cases of one of I_{IN}, I_{SH}, I_{EX} dominating the current noise give closed solutions and are of particular interest.

CASE 1. $I_{EX}, I_{IN} \approx 0$.

This is the case of shot noise limited noise, particularly relevant when photomultiplier tubes are used. We find the optimal A_o to be given by

$$A_o = \frac{1}{\eta} \log_{10} \frac{1+\eta}{1-\eta} \quad . \tag{3.8}$$

Figure 3.3 is a plot of the optimal A_o vs. η. It is useful to note that in the limit of small changes ($\eta << 1$), the optimal A_o is given by

$$A_o\Big|_{\eta << 1} = \frac{2}{2.303} + O(\eta))$$

$$" \quad = 0.868 \ldots$$

---

[13] For example, if the optical density exponentially recovers in time, $\eta = \eta_0\, e^{-t/\tau}$, where η_0 determines the amount of bleaching at $t = 0$ and τ is the recovery time constant.

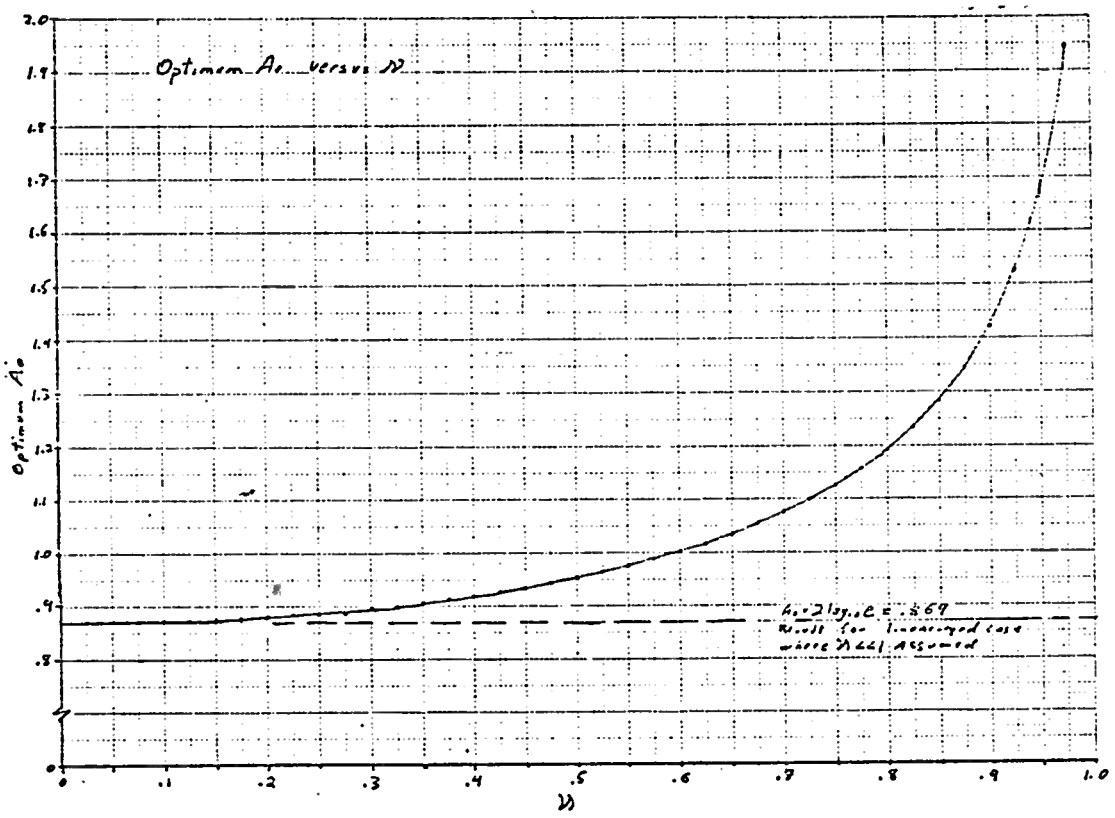

Figure 3.3

When the optimum sample A_0 is chosen, the $\delta S/N$ becomes:

$$\left.\frac{\delta S}{N}\right|_{A_0=\text{optimum } A_0} = \sqrt{\frac{\mathcal{R}P_0}{2e\Delta\nu}} \quad 2\mathcal{N}\left[\frac{(1-\mathcal{N})^{1-\mathcal{N}}}{(1+\mathcal{N})^{1+\mathcal{N}}}\right]^{1/2\mathcal{N}} \tag{3.9}$$

This is plotted as a function of $\mathcal{N}$ in Figure 3.4. The following limiting cases are of interest:

$$\left.\frac{\delta S}{N}\right|_{\substack{\mathcal{N}=1 \\ A_0=\text{Optimal } A_0(=\infty)}} = \sqrt{\frac{\mathcal{R}P_0}{2e\Delta\nu}}$$

$$\left.\frac{\delta S}{N}\right|_{\substack{\mathcal{N}\ll 1 \\ A_0=\text{Optimal } A_0(=.868)}} = \sqrt{\frac{\mathcal{R}P_0}{2e\Delta\nu}}\ \mathcal{N}$$

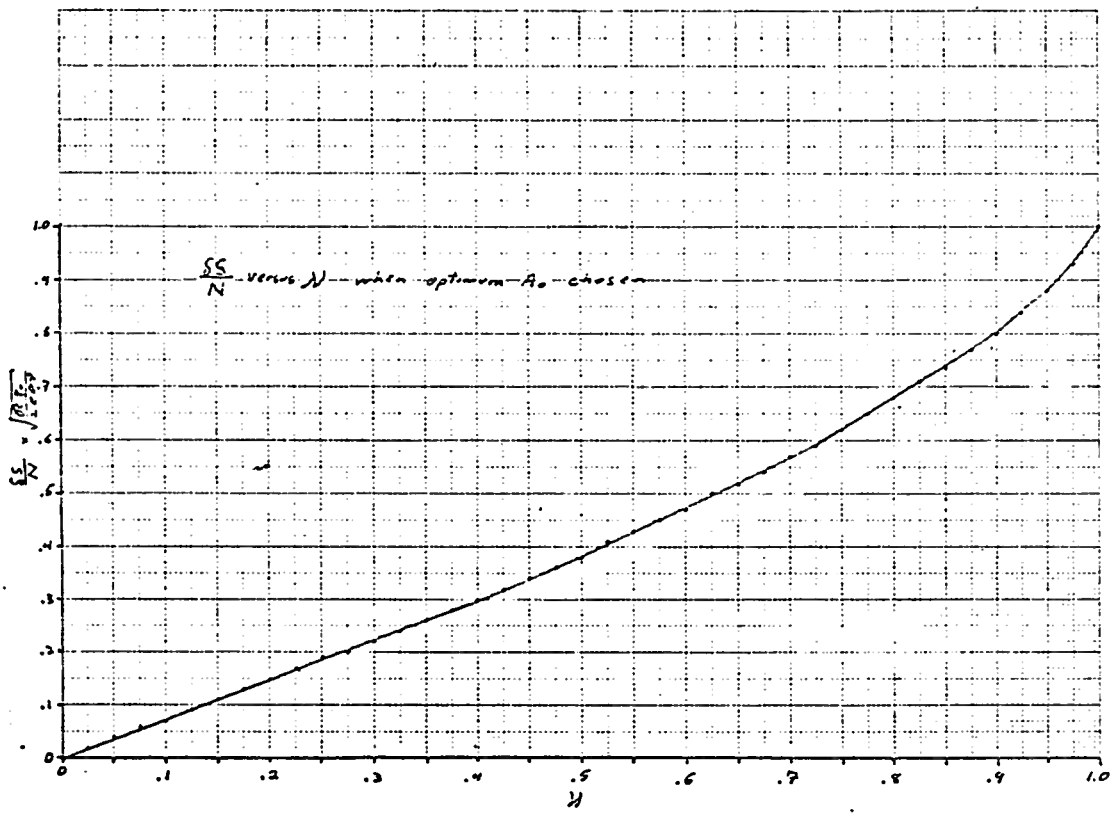

Figure 3.4

The sensitivity of the $\delta S/N$ to A_0 is of interest, as it tells us how far away from the optimal A_0 we can work without substantial loss in $\delta S/N$. This may be particularly important if only limited amounts of a sample can be obtained, or, if the actinic light cannot adequately penetrate the sample, preventing complete optical bleaching. Figure 3.5 is a plot of $\delta S/N$ vs. A_0 for various η. We are clearly more sensitive to loss in $\delta S/N$ for A_0's below the optimal A_0 than for those above.

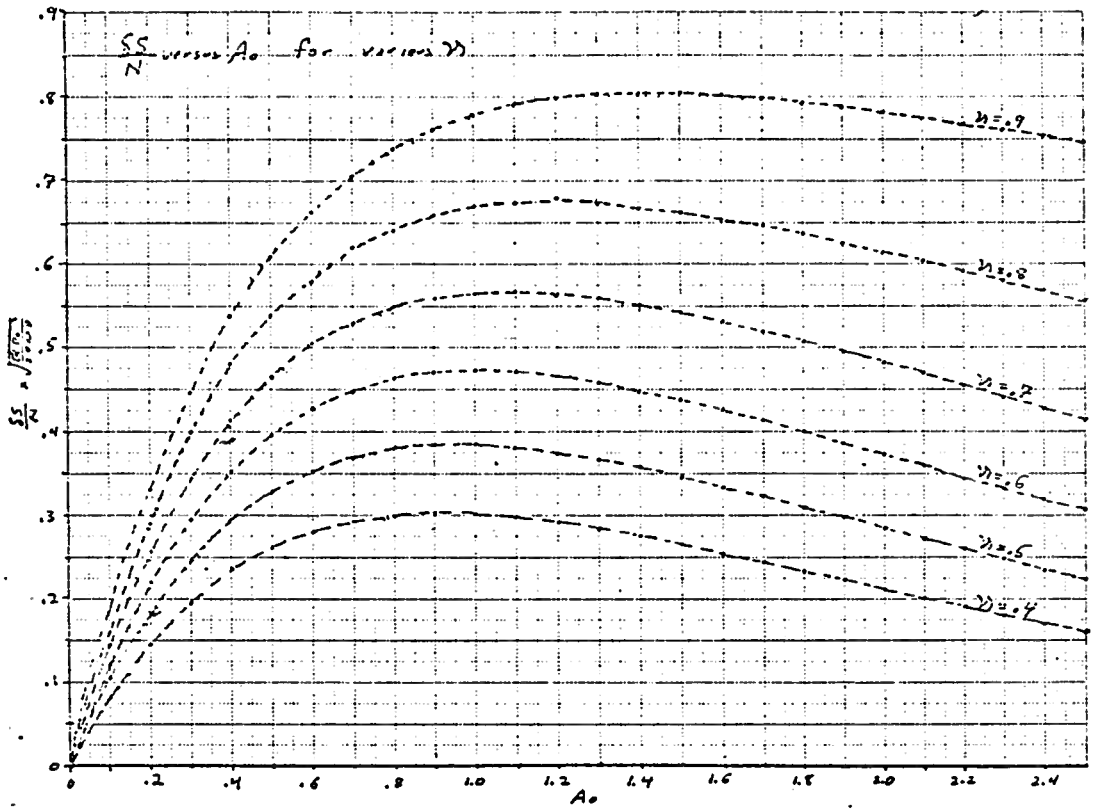

Figure 3.5

CASE 2., I_{SH}, $I_{EX} \simeq 0$.

This is the case where detection is limited by non-shot noise sources, such as photodetector-dark current or amplifier noise. We find that the optimal A_0 is given by:

$$A_0\Big|_{\text{Optimal}} = \frac{1}{\nu} \log_{10} \frac{1}{1-\nu} . \qquad (3.10)$$

Figure 3.6 is a plot of the optimal A_0 v.s. ν. In the limit of small absorbance changes ($\nu \ll$), the optimum A_0 is given by

$$A_0 = 1/2.3 + 0(\nu)$$

$$" = 0.434...$$

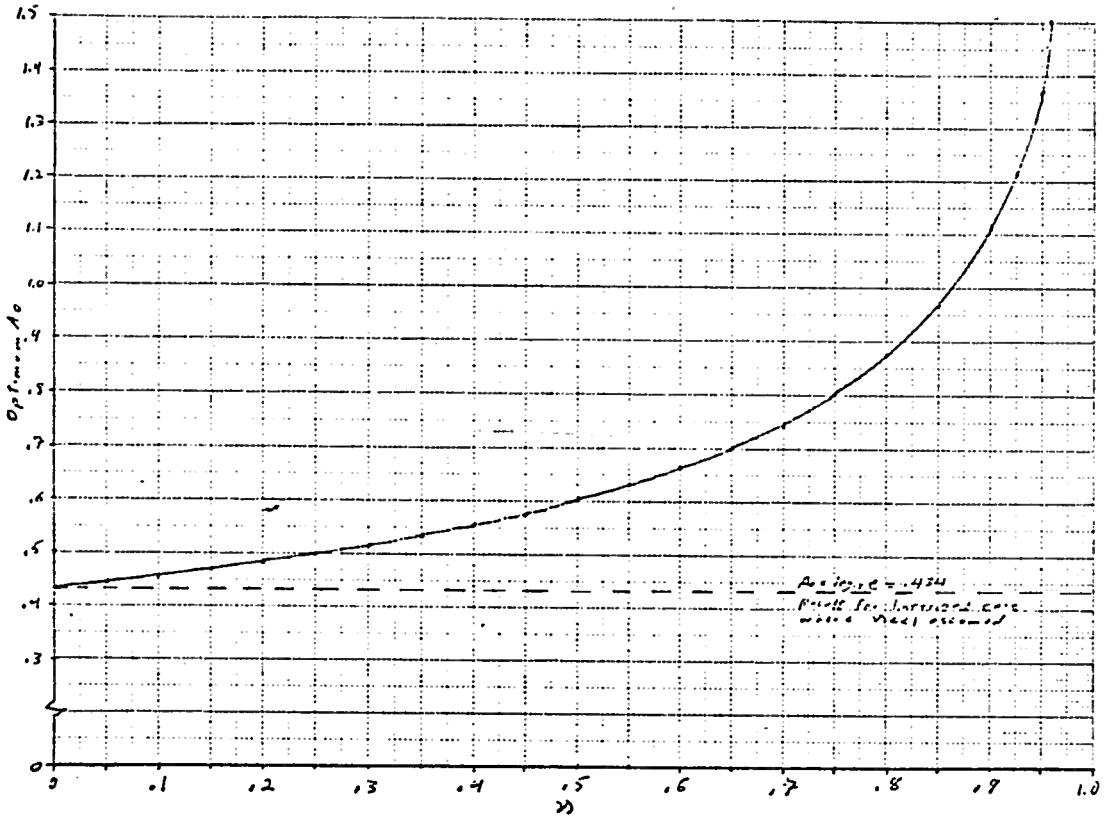

Figure 3.6

When the optimum sample A_0 is chosen, the $\delta S/N$ becomes:

$$\left.\frac{\delta S}{N}\right|_{A_0=\text{Optimum } A_0} = \sqrt{\frac{\mathcal{R}P_0}{I_{EX}}}\ \eta\left[(1-\eta)^{1-\eta}\right]^{1/\eta} \quad . \tag{3.11}$$

This is plotted as a function of η in Figure 3.7. For the limiting cases of $\eta=1$ and $\eta<<1$, we have

$$\left.\frac{\delta S}{N}\right|_{\substack{\eta=1\\ A_0=\text{Optimal } A_0(=\infty)}} = \sqrt{\frac{\mathcal{R}P_0}{I_{IN}}}$$

$$\left.\frac{\delta S}{N}\right|_{\substack{\eta<<1\\ A_0=\text{Optimal } A_0(=.434)}} = \sqrt{\frac{\mathcal{R}P_0}{I_{IN}}}\ \eta$$

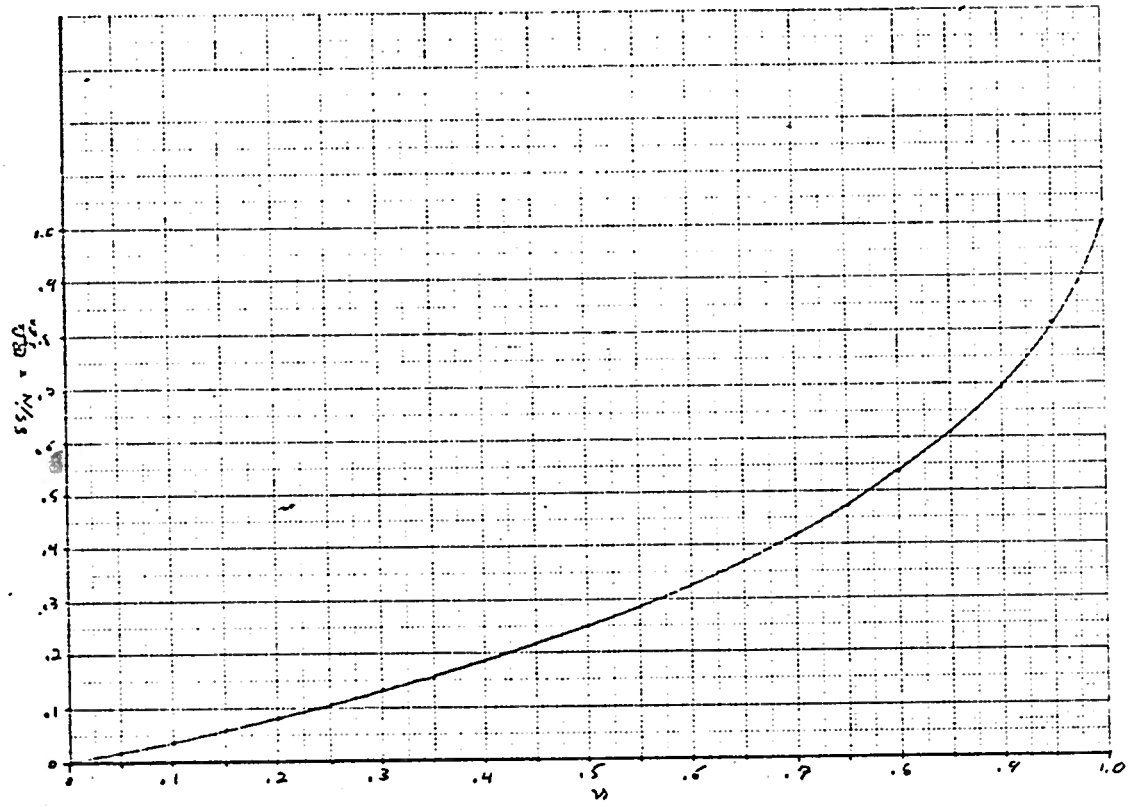

Figure 3.7

Figure 3.8 is a plot of $\delta S/N$ vs. A_0 for various η in order to demonstrate the sensitivity of $\delta S/N$ to nonoptimal A_0.

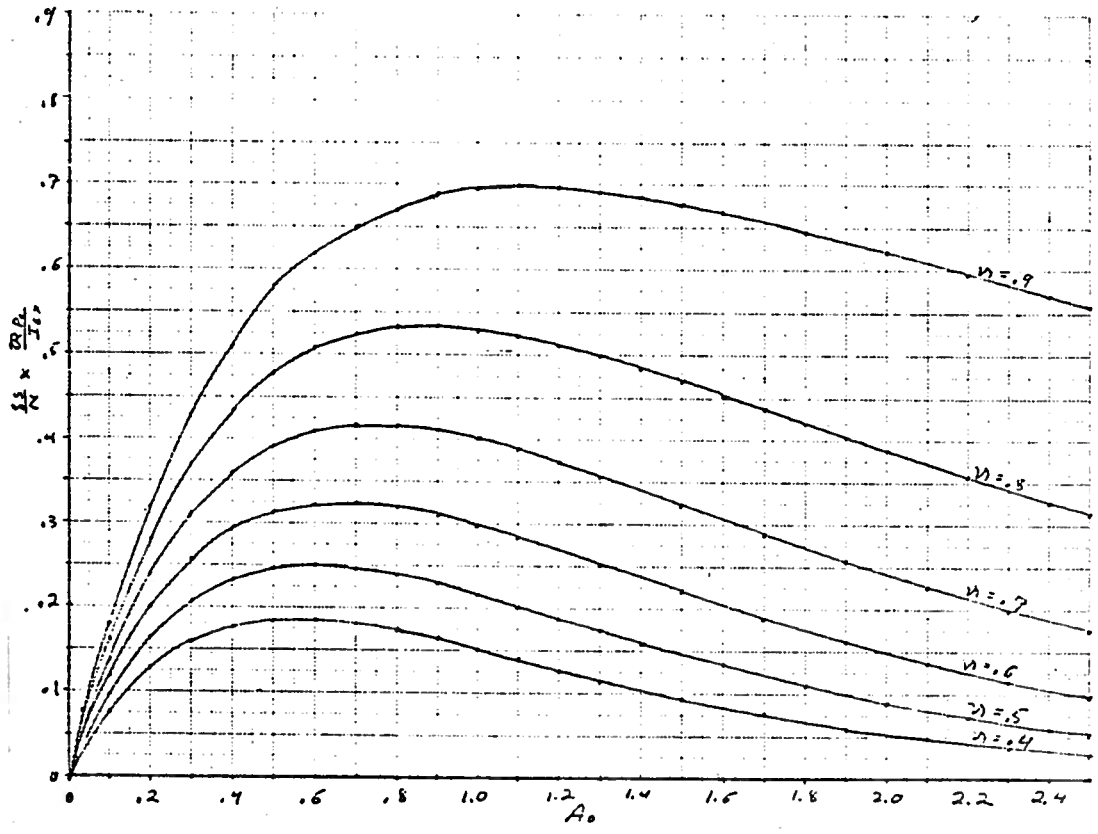

Figure 3.8

CASE 3, I_{SH}, $I_{IN} \simeq 0$.

This case is applicable to photodetection with PIN photodiodes where the total noise is limited by the low-frequency excess noise of the photodiode. Because both the signal and the noise are proportional to P, the $\delta S/N$ depends only on the change in sample absorbance, not the initial absorbance. Specifically,

$$\frac{\delta S}{N} = \frac{1 - e^{-2.3\ \delta A}}{\alpha(f)} \quad . \tag{3.12}$$

The optimum A_0 is clearly independent of η and given by $A_0 \to \infty$. "∞" can be interpreted as $A_0 >> 1/2.3\eta$. Unlike the previous two cases, this requires the largest A_0 when η is very small. For example, we need $A_0 >> 20$ for $\eta = .1$, $A_0 >> .5$ for $\eta = .85$ and $A_0 >> .4$ for $\eta = 1$.

Figure 3.9 is a plot of $\delta S/N$ versus A_0 for various η.

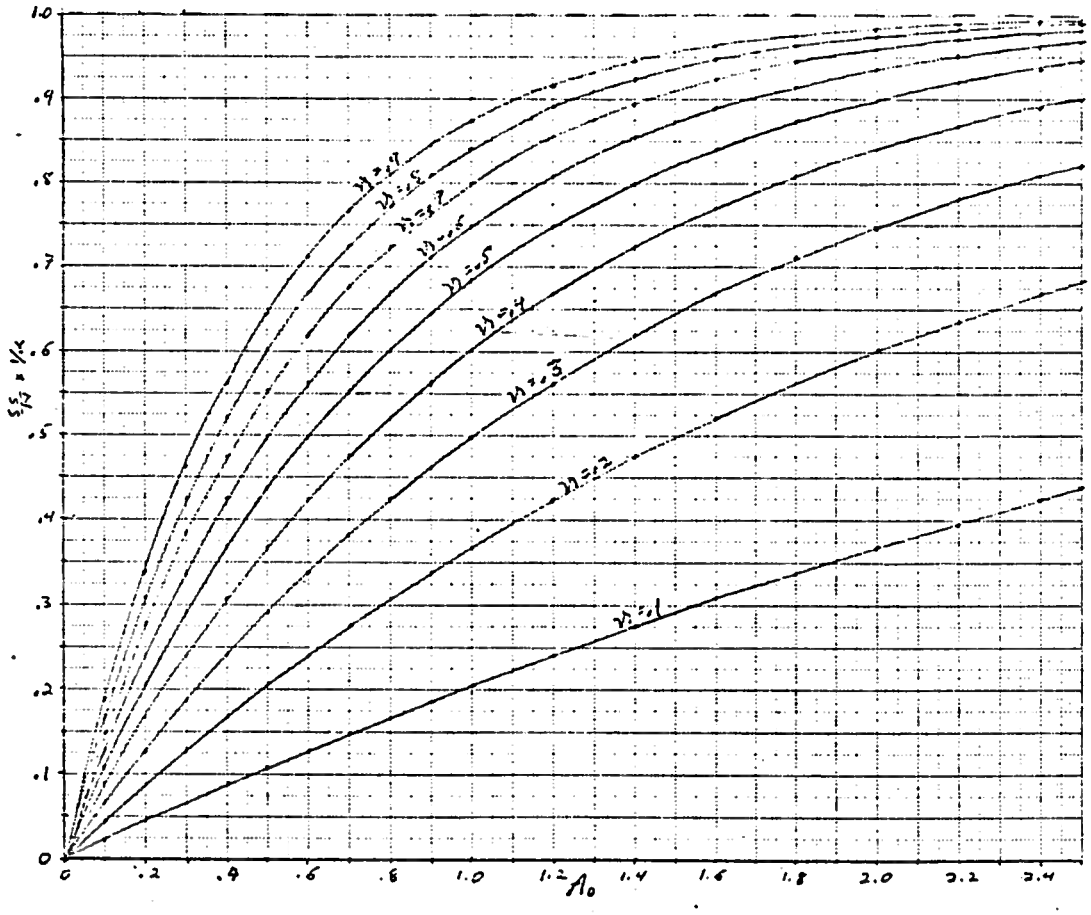

Figure 3.9

Remarks on Photodetectors

The conclusions as whether to use a photomultiplier tube on a photodiode are in part very similar to those reached in the previous section. If events change slowly in time (< 100 Hz), we have to balance the increased responsivity of the diode against its low-frequency excess noise characteristics. Again, the use of phase sensitive detection may be of use in getting out of the low-frequency region. It must be noted that optimal sample A_0's are much greater for the excess noise limited case than the shot noise limited case. Practically, this means that working in the shot noise limit requires less sample material.

At high speeds (> 1000 Hz), both photomultiplier tubes and photodiodes are shot noise limited. On that basis, photodiodes should be preferable due to their higher responsivity. We will see, however, in Section IV that this advantage may be removed due to noise amplified by the photodiodes junction capacitance, in the current-to-voltage amplifiers that must follow the photodiode. As will be discussed in more detail later, it appears that photomultiplier tubes are more practically suited for measuring time varying signals on a constant background.

As an illustration of calculating the $\delta S/N$ in a flash photolysis experiment employing a photomultiplier tube, Eq. (3.6) in the shot noise limit ($I_{IN} \simeq I_{EX} \simeq 0$) was applied to a laboratory situation. Including the partition noise prefactor, we have, after rearrangement

$$\frac{\delta S}{N} = \sqrt{\frac{g-1}{g}} \sqrt{\frac{2\mathcal{R}P}{e\Delta\nu}} \sinh\left(\frac{2.3}{2}\,\eta\, A_0\right) \qquad (3.13)$$

where $P = P_0 e^{-2.3 A_0}$.

As a sample, we used reaction centers from Rhodopseudomonas sphaeroides R-26 with $A_0(805\text{ nm}) = 0.34$ and $\eta = .9$. The monitoring beam was set at $\lambda = 865$ nm and $P_0 = 22$ nW. The photomultiplier tube was a Hammamatsu R955 with $\mathcal{R} = .0051$ A/W and $G = 5$. From Eq. (3.13) we calculate $\delta S/N = 12$. Figure 3.10 shows the actual

response on the system in response to an actinic flash. From the data we find $\delta S/N \simeq 12$. The excellent agreement with theory should not be taken too seriously, but the ability to predict $\delta S/N$ is well illustrated.

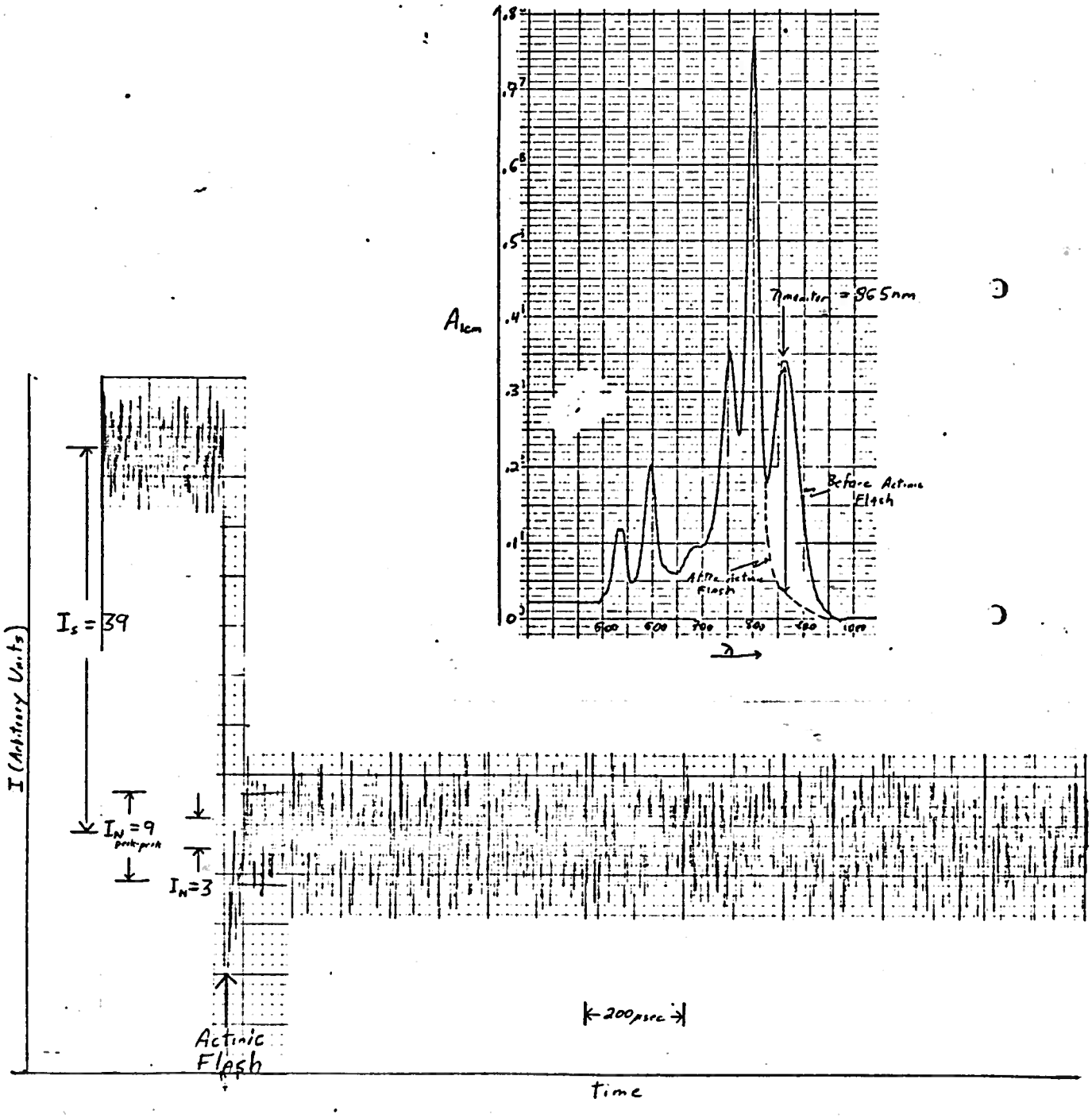

Figure 3.10

IV Noise in Operational Amplifiers

Photomultipliers have built-in amplifiers, the dynode structure, and the effect of the dynodes on the S/N has already been discussed. Still, for sufficiently small anode currents, the external amplifier may affect the S/N. Photodiodes must always be used with an external amplifier and in many important cases the S/N of the photodiode photodetector system is limited by the amplifier. As operational amplifiers are well suited for use in photodetector systems, we will explore their noise characteristics in detail.

I will model the real operational amplifier (op-amp) as an ideal operational amplifier[14] with voltage noise sources, e_n, and current noise sources, i_n, represented phenomenologically as input supplies. See Figure 4.1

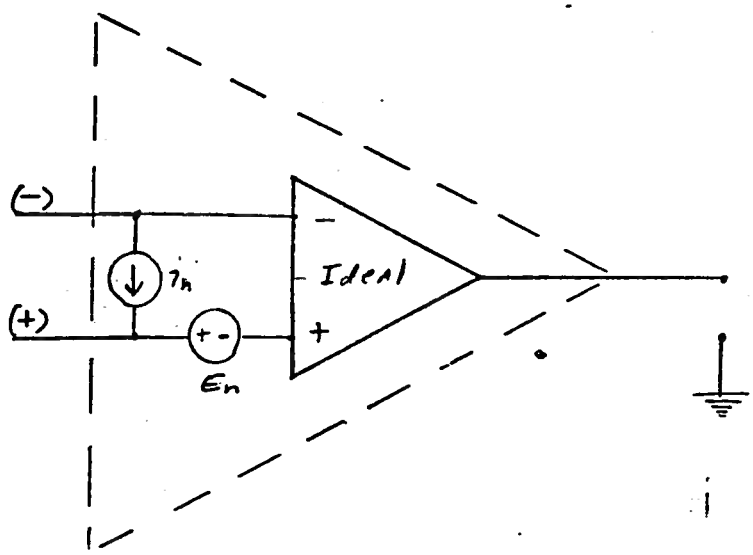

Figure 4.1

The voltage (current) noise source has units of Volts (Amps) per $\sqrt{Hz}$.

[14]This assumes an infinite input impedance, Z_i, zero output impedance, Z_o, and an infinite open loop gain, $A(\omega)$, at all frequencies. In practical terms, the first condition requires that Z_i (typically $10^6\Omega$ to $10^{15}\Omega$ for some FET op-amps) is much greater than the chosen feedback impedance. The second condition requires that Z_o be much smaller than the impedance of the device following the op-amp, or equivalently, that very little output current is drawn (typically < 5 mA). The third condition demands that we work at a bandwidth below the op-amp unity gain bandwidth, the frequency at which $A(\omega) = 1$ (as high as 70 MHz for some amplifiers).

The values of i_n, the op-amp current noise, and e_n, the op-amp voltage noise can easily be measured as a function of frequency. They are also usually specified by manufacturers. To measure them, I connected feedback impedance, Z_f, with both variable feedback resistance, R_f, and capacitance, C_f, between the (-) input terminal and the output terminal of the op-amp. Note that the feedback impedance will contribute Johnston noise. The output of the op-amp is connected to the noise measuring setup consisting of a lock-in detector followed by a true RMS voltmeter, described earlier. The circuit for this setup, including noise sources, is shown in Figure 4.2.

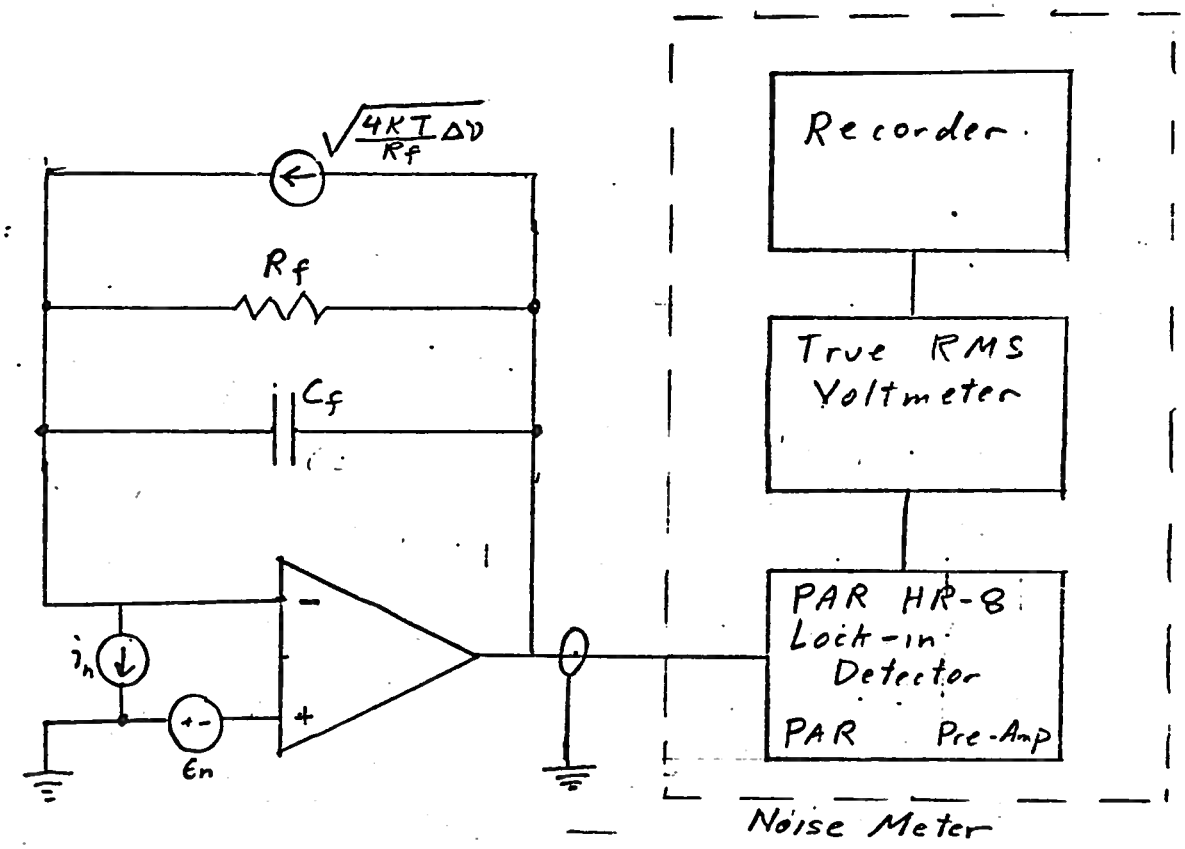

Figure 4.2

The output voltage, E_N, from the feedback op-amp is due purely to its noise sources, and is given by:

$$E_N\Big|_{Z_{input}=\infty} = \sqrt{\left[e_n^2 + |Z_f|^2\left(i_n^2 + \frac{4kT}{R_f}\right)\right]\Delta\nu} \qquad (4.1)$$

where $|Z_f| = R_f/\sqrt{1 + (\omega R_f C_f)^2}$.[15] $\Delta\nu$ is the bandwidth, chosen as 1 Hz for all measurements. C_f has a lower limit of a few picofarads due to stray capacitances in connecting leads, etc. For the op-amp mount used, the stray capacitance was measured to be 6.7 pF. For $R_f < 30$ KΩ, the op-amps tested tended to oscillate at a few MHz, requiring larger (12-30 pF) C_f's. In general, it was best to choose C_f such that $|Z_f| \simeq R_f$. From Eq. (4.1) we see that for small R_f, $E_N \approx e_n \sqrt{\Delta\nu}$ and that for large R_f, $E_N \approx R_f i_n \sqrt{\Delta\nu}$. Thus, a fit of experimental data of E_N versus R_f will yield the values of e_n and i_n. This is shown for the AD146C op-amp at 100 Hz in Figure 4.3 The dots are measured data points and the dotted line the fit to Eq. (4.1) with $e_n = 110$ nV/$\sqrt{\text{Hz}}$ and $i_n = 42$ fA/$\sqrt{\text{Hz}}$. This measurement procedure was undertaken at a number of points in the frequency range 10-10^4 Hz for both the AD147C and AD528J amplifiers. Both of these are high input

---

[15]Expression (4.1), as well as future expressions giving the noise or S/N for a system, contain ω implicitly and must be properly evaluated for the bandwidth of interest. Essentially, for a bandwidth $\Delta\nu = \nu_2 - \nu_1$, we integrate e_o^2 over the bandwidth to find the total noise voltage. To illustrate, we have

$$E_N\Big|_{\substack{Z_{input}=\infty \\ Total}} = \sqrt{\int_{2\pi\nu_1}^{2\pi\nu_2} \left[e_n^2 + \frac{R_f^2 i_n^2 + 4kT R_f}{1 + (\omega R_f C_f)^2} \right] \frac{d\omega}{2\pi}}$$

$$" = \sqrt{e_n^2 \Delta\nu + \frac{R_f^2 i_n^2 + 4kT R_f}{2\pi R_f C_f} \left[\tan^{-1}(2\pi\nu_2 R_f C_f) - \tan^{-1}(2\pi\nu_1 R_f C_f) \right]}$$

For $\nu_1 < \nu_2 << \frac{1}{2}\pi C_f R_f$, this reduces to the simple case:

$$E_N\Big|_{\substack{Z_{input}=\infty \\ Total}} = \sqrt{(e_n^2 + i_n^2 R_f^2 + 4kT R_f)\,\Delta\nu}$$

In expressions where the noise voltage is a rather complicated or messy function of ω, such as 4.2, it is often easier to do the integration numerically.

TABLE 4.1

	AD147C[1] (FET)		AD528J[2] (FET)	
	$Z_i = 10^{12}\Omega$ BW = 10 MHz		$Z_i = 10^{12}\Omega$ BW = 10 MHz	
Frequency	e_n	i_n	e_n	i_n
10 Hz	190 nV/$\sqrt{Hz}$	fA/$\sqrt{Hz}$	180 nV/$\sqrt{Hz}$	40 fA/$\sqrt{Hz}$
30 "	130 "	"	-	-
100 "	110 "	42 "	160 "	27 "
300 "	68 "	"	-	-
1 KHz	40 "	"	160 "	∿ 15 "
3 "	33 "	"	-	-
10 "	∿ 50 "	"	160 "	∿ 400 "

[1]Manufacturer specifies e_n (.01 Hz to 1 Hz, p-p) = 3 μV

e_n (5 Hz to 50 KHz, r.m.s.) = 12 μV

i_n (.01 to 1 Hz, p-p) = 0.1 pA

[2]Manufacturer specifies e_n (.1 Hz to 10 Hz, p-p) = 5 μV

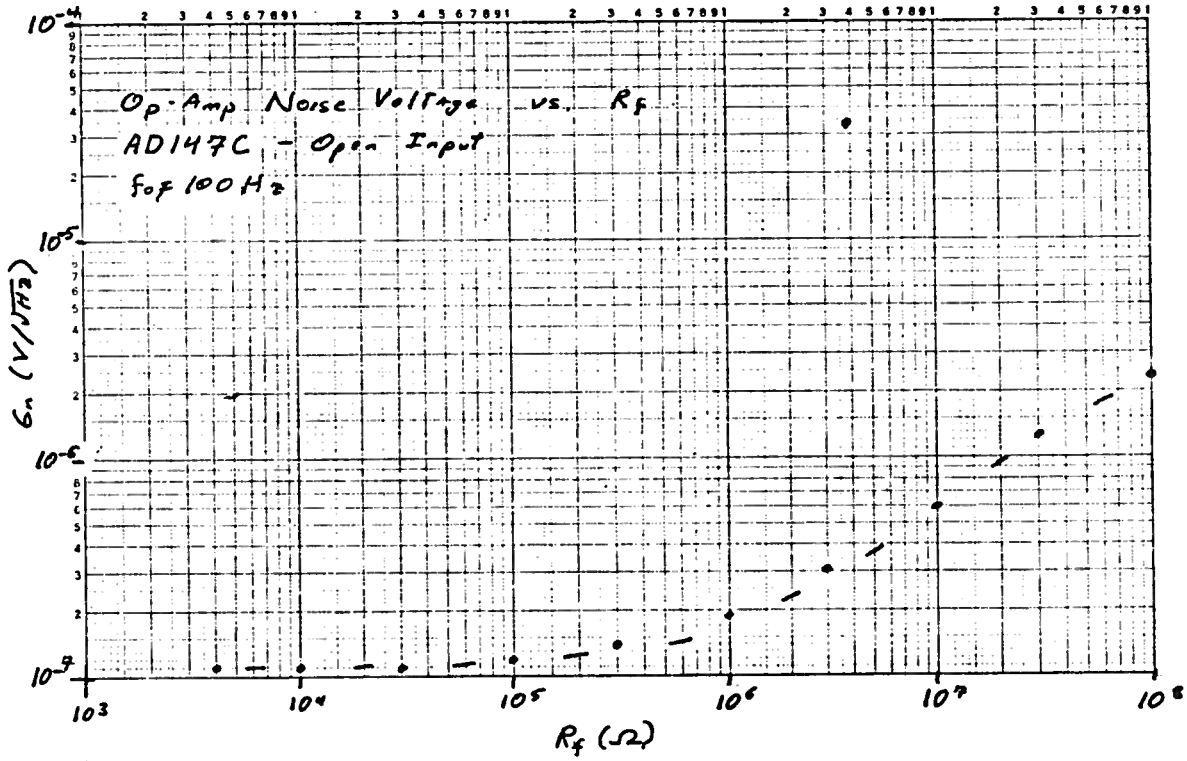

Figure 4.3

impedance, high speed (> 1 MHz) FET op-amps. The results are shown in Table 4.1. The rise in noise levels near 10 Hz is probably due to "1/f" noise contributions. The manufacturer's typical noise level ratings were incomplete for both amplifiers. However, the measured values comply with the limited data given. Table 4.2 is a listing of medium to high speed, low noise op-amps possibly suitable for use in photodetector systems. It does not include information on phase variation versus frequency, input offset currents and long-term offset current drift, which may be of relevance. Further, it is possible to use a low noise dual JFET as an input buffer to an op-amp to construct an extremely low noise amplifier.[16] Typical designs give e_n = 6 nV/$\sqrt{Hz}$ at 10 Hz and an integrated noise voltage of 190 nV and an integrated current noise of 62 fA over the range 1 Hz to 1 KHz. The

---

[16]"Designing Junction FET Input Op-Amps', Siliconix Incorporated, Application Note AN74-3.

unity gain - open loop bandwidth is limited to ∿ 800 KHz by the JFET input capacitance. Slow rates will be quite small (typically < 1 V/usec) making these amplifiers suitable only for small signals.

Equation (4.1) also describes how the noise output varies with frequency due to the feedback impedance. Consider a bandwidth where e_n and i_n are approximately constant (f > 10 Hz) and take R_f large for convenience. At low frequency the noise is current limited (i.e., $E_N \approx R_f i_n \sqrt{\Delta\nu}$). As the frequency increases towards $2\pi/R_fC_f$, the noise falls off as $1/\omega$ until the output reaches a voltage noise limited (i.e., $E_N \approx e_n \sqrt{\Delta\nu}$) plateau. This is shown in Figure 4.4 for the AD147C op-amp. The rise in measured noise at the highest frequency is due to a small, ∿ 1-3 pF, stray input capacitance. Of course, the signal will also fall off for $f > 2\pi/R_fC_f$.

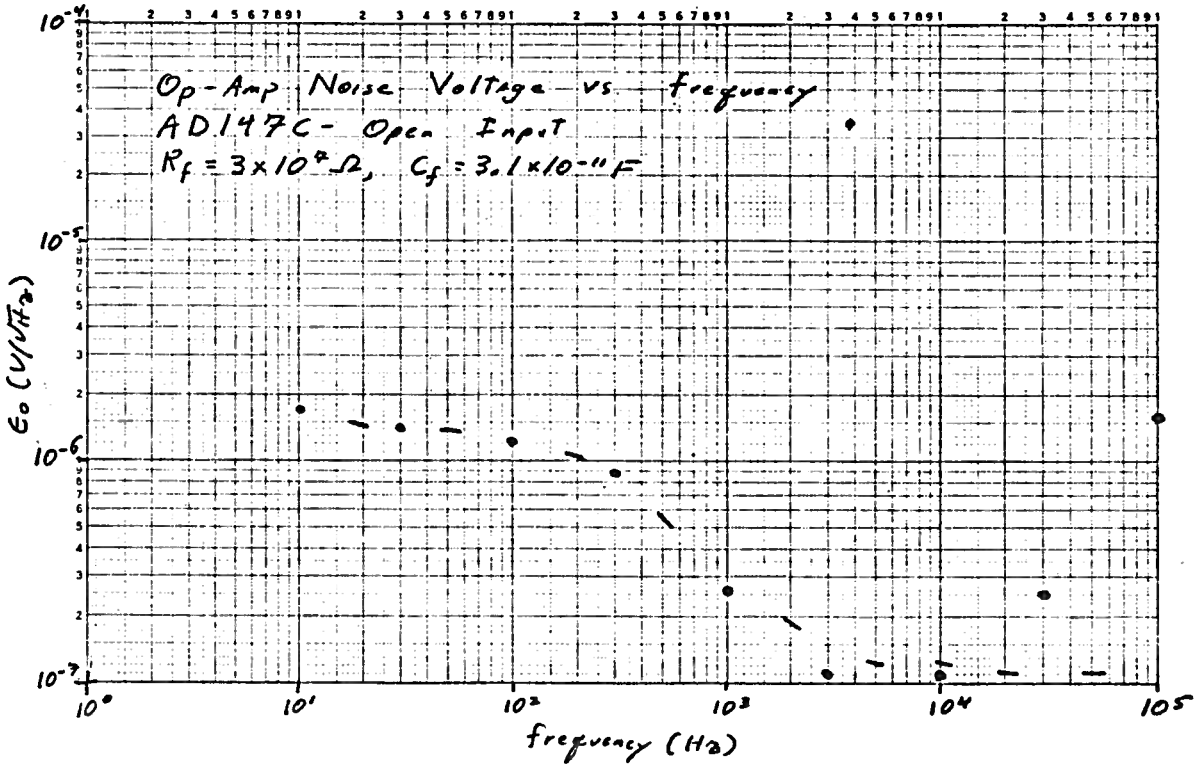

Figure 4.4

TABLE 4.2

	AD507		AD509		OP16	
	$Z_i = 10^8\Omega$; BW = 35 MHz[1]		$Z_i = 10^8\Omega$; BW = 20 MHz[1]		$Z_i = 10^{12}\Omega$; BW = 8 MHz	
Frequency (Hz)	$e_n(nV/\sqrt{Hz})$	$i_n(fA/\sqrt{Hz})$	$e_n(nV/\sqrt{Hz})$	$i_n(fA/\sqrt{Hz})$	$e_n(nV/\sqrt{Hz})$	$i_n(fA/\sqrt{Hz})$
10^0	-	-	-	-	-	-
10^1	100	-	100	-	50	-
10^2	30	-	30	-	20	10
10^3	19	-	19	-	15	10
10^4	-	-	-	-	15	-
10^5	12	-	12	-	-	-

	LF356		LF355		μA739	
	$Z_i = 10^2\Omega$; BW = 4.5 MHz		$Z_i = 10^{12}\Omega$; BW = 2.5 MHz		$Z_i = 10^5\Omega$; BW = 1 MHz	
Frequency (Hz)	$e_n(nV/\sqrt{Hz})$	$i_n(fA/\sqrt{Hz})$	$e_n(nV/\sqrt{Hz})$	$i_n(fA/\sqrt{Hz})$	$e_n(nV/\sqrt{Hz})$	$i_n(fA/\sqrt{Hz})$
10^0	-	-	-	-	-	-
10^1	60	-	90	-	8	3200
10^2	15	10	25	10	6	1300
10^3	12	10	25	10	5	630
10^4	12	-	25	-	5	320
10^5	12	-	25	-	5	320

	OP07		AD52		AD515	
	$Z_i = 10^8\Omega$; BW = 600 KHz		$Z_i = 10^{12}\Omega$; BW = 500 KHz		$Z_i = 10^{15}\Omega$; BW = 350 KHz	
Frequency (Hz)	$e_n(nV/\sqrt{Hz})$	$i_n(fA/\sqrt{Hz})$	$e_n(nV/\sqrt{Hz})$	$i_n(fA/\sqrt{Hz})$	$e_n(nV/\sqrt{Hz})$	$i_n(fA/\sqrt{Hz})$
10^0	-	-	70	7	[4.0μV(p-p) 0.1-10 Hz]	[3.0 fA(p-p) 0.1-10 Hz]
10^1	10.3	320	25	2.5	75	
10^2	10.0	140	20	3.5	55	[100fA
10^3	9.6	120	13	6	50	10 Hz to 10 KHz]
10^4	-	-	-	-	-	
10^5	-	-	-	-	-	-

[1]These op-amps require external compensation to be used as current to voltage converters, and this will lower the effective BW to 10-12 MHz.

I will now consider the effect of input impedance on the op-amps noise output. The circuit for the case of a parallel R-C input impedance, corresponding to an unbiased photodetector in the dark, is shown in Figure 4.5. The op-amp noise output voltage becomes

$$E_N = \sqrt{\left[\left|1 + \frac{Z_f}{Z_i}\right|^2 e_n^2 + |Z_f|^2 \left(i_n^2 + \frac{4kT}{R_f} + \frac{4kT}{R_i}\right)\right] \Delta\nu} \qquad (4.2)$$

where

$$\left|1+\frac{Z_f}{Z_i}\right| = \sqrt{\frac{\left\{1+(\omega R_f C_f)^2 + \left(\frac{R_f}{R_i}\right) 1+(\omega R_i C_i)(\omega R_f C_f)\right\}^2 + \left\{\left(\frac{R_f}{R_i}\right)\omega(R_i C_i - R_f C_f)^2\right\}^2}{1+(\omega R_f C_f)^2}}$$

Equation (4.2) shows that for finite input impedance, the input voltage noise of the op-amp is amplified. The dependence of e_o on R_i is illustrated in Figure 4.6 for the AD147C op-amp, where ω, C_i, and C_f were chosen to insure

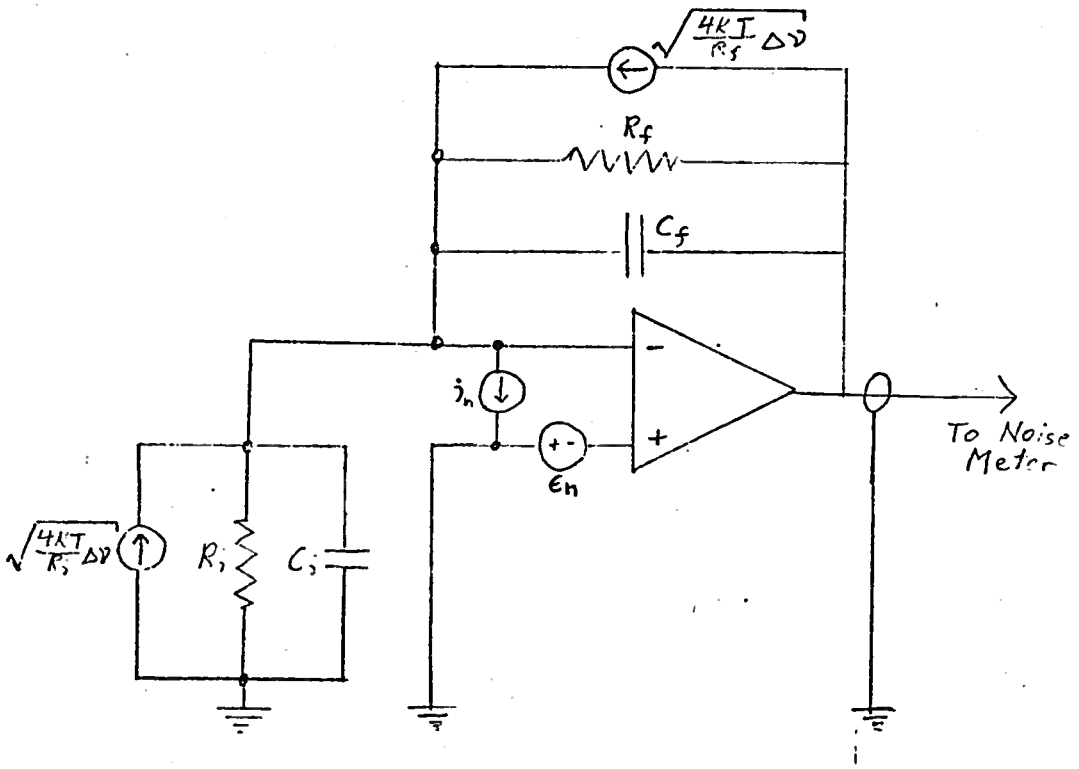

Figure 4.5

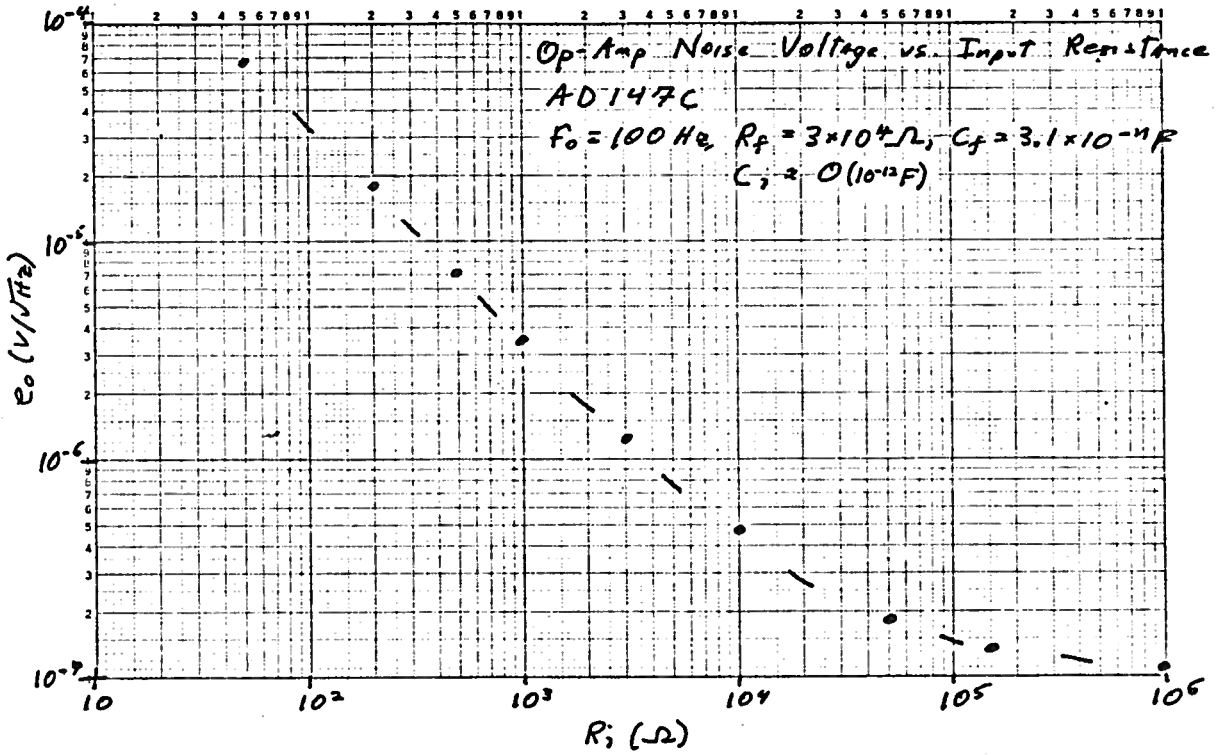

Figure 4.6

$|1 + Z_f/Z_i| \approx [1 + R_f/R_i]$. Equation (4.2) also illustrates that for finite input capacitance, the amplifier output noise will increase with frequency. When using an op-amp with a photodetector the conditions $\omega R_f C_f << 1$ and $R_f << R_i$ usually hold. For this case, Eq. (4.2) simplifies to

$$\left|1 + \frac{Z_f}{Z_i}\right| \approx \sqrt{1 + \left(1 + 2\,\frac{C_f}{C_i}\right)\,(\omega R_f C_i)^2 + \left(\frac{C_f}{C_i}\right)^2\,(\omega R_f C_i)^4}$$

This illustrates the need to keep the detector capacitance small when working at high frequencies. We will illustrate this point for photodiode detector systems in the next section.

It is worth examining the S/N of an op-amp for various common configurations in the limit of negligible input source noise. This will improve our intuition for S/N calculations and is useful for setting upper limits the S/N attainable with op-amp containing circuits.

Case 1

Current to voltage converter:

$$S/N = \frac{Z_f I_i}{\sqrt{\left[\left|1 + \frac{Z_f}{Z_i}\right|^2 e_n^2 + |Z_f|^2 \left(i_n^2 + \frac{4kT}{R_f} + \frac{4kT}{R_i}\right)\right] \Delta\nu}} \tag{4.3}$$

where I_i is the input current. We see that the S/N increases as $Z_f \to \infty$. For a common situation, $Z_i >> Z_f$, the S/N increases roughly linear with Z_f, the conversion gain, from a voltage noise limited value of

$$S/N\Big|_{Z_i >> Z_f} \approx \frac{Z_f I_i}{e_n \sqrt{\Delta\nu}} \qquad Z_f << e_n/i_n$$

to a current noise limited value of

$$S/N\Big|_{Z_i >> Z_f} \approx \frac{I_i}{i_n \sqrt{\Delta\nu}} \qquad Z_f >> e_n/i_n$$

which is independent of Z_f. For this situation, it is clearly best to keep $Z_f >> e_n/i_n$ if bandwidth considerations allow so.

Case 2

Inverting voltage amplifier

$$S/N = \frac{|Z_f/Z_i| V_i}{\sqrt{\left[\left|1 + \frac{Z_f}{Z_i}\right|^2 e_n^2 + |Z_f|^2 \left(i_n^2 + \frac{4kT}{R_f} + \frac{4kT}{R_i}\right)\right] \Delta\nu}} \tag{4.4}$$

where V_i is the input voltage. We see that the S/N increases as $Z_f \to \infty$ or $Z_i \to 0$. In the limit of low-voltage gain, $|Z_f/Z_i| \ll 1$, the S/N is voltage noise limited to

$$S/N \approx \left|\frac{Z_f}{Z_i}\right| \frac{V_i}{e_n\sqrt{\Delta\nu}}$$

In the high voltage gain, $|Z_f/Z_i| \gg 1$, the S/N increases until the limited

$$S/N \approx \frac{V_i}{\sqrt{\left[e_n^2 + |Z_i|^2\left(i_n^2 + \frac{4kT}{R_i}\right)\right]\Delta\nu}}$$

which is independent of the voltage gain. In this limit, the S/N is maximized for $Z_i \ll e_n/i_n$.

Case 3

Noninverting voltage amplifier

$$S/N = \frac{|1 + Z_f/Z_i|\, V_i}{\sqrt{\left[\left|1 + \frac{Z_f}{Z_i}\right|^2 e_n^2 + |Z_f|^2\left(i_n^2 + \frac{4kT}{R_f} + \frac{4kT}{R_i}\right)\right]\Delta\nu}} \quad . \qquad (4.5)$$

In the limit of unity voltage gain, $|Z_f/Z_i| \ll 1$, the S/N is:

$$S/N \approx \frac{V_i}{\sqrt{\left[e_n^2 + |Z_f|^2\left(i_n^2 + \frac{4kT}{R_f}\right)\right]\Delta\nu}}$$

In this limit, the S/N is maximized for $Z_f \ll e_n/i_n$. In the limit of high voltage gain, $|Z_f/Z_i| \gg 1$, the S/N is:

$$S/N \quad \frac{V_i}{\sqrt{e_n^2 + |Z_i|^2 \left(i_n^2 + \frac{4kT}{R_i}\right) \Delta\nu}}$$

In this limit, the S/N is maximized for $Z_i \ll e_n/i_n$. Note that in both limits the S/N is independent of the voltage gain, and will in fact have the same voltage noise limiting value of

$$S/N = \frac{V_i}{e_n\sqrt{\Delta\nu}}$$

if Z_i, $Z_f \ll e_n/i_n$ and Z_i, $Z_f \gg 4kT$.

V. Photodetector System Design

We have discussed separately the noise and S/N of photomultiplier tubes, photodiodes and operational amplifiers. The complete photodetector system requires a photodetector followed by an amplifier. The noise of these two devices will, at the minimum, add as the square root of the sum of the squares while the finite impedance of the devices will lead to amplification of the op-amp voltage noise, decreasing the overall S/N. The photodetector impedance is essentially capacitive and will be discussed purely in that regard.

Photodetector Capacitance and Noise.

In Section IV we discussed the effect of finite input impedance on the noise output of op-amps. From Eq. (4.2), we see that we have a noise contribution to the op-amp output voltage, after reasonable simplification, given by

$$E_N^2 \approx \left[1 + \left(1 + \frac{2\,C_f}{C_i}\right)(\omega R_f C_i)^2 + \left(\frac{C_f}{C_i}\right)^2 (\omega R_f C_i)^4\right] e_n^2\,\Delta\nu\ .$$

For the special but often useful case of $C_f << C_i$, the total noise voltage is:

$$E_N^2 \approx [(\text{constant})^2 + (\omega R_f C_i e_n)^2] \Delta\nu \ . \qquad (5.1)$$

This particular case is easy to test experimentally, as we expect the op-amp noise voltage to increase linearly with frequency after a certain plateau region. Such a test was done using a photodetector system consisting of a UDT 10-D photodiode and a AD147C op-amp in conjunction with a Federal Scientific UQ-10 Spectrum Analyzer. The results, plotted as noise voltage versus frequency, are shown in Figure 5.1. Three different curves are present representing different values of photodiode capacitance. The photodiode capacitance is adjustable by the application of a reverse bias potential to the photodiode, a topic I will discuss later. From the data, we can work backward using Eq. (5.1) and calculate the values of C_i (the photodiode junction capacitance) for the different reverse bias levels. The capacitance values (given in Figure 5.1) are slightly higher than the typical values specified by the manufacturer. An attempt to measure the capacitance of the photodiode directly with a grid dip meter met with failure. However, the problems associated with photodetector capacitance are well illustrated.

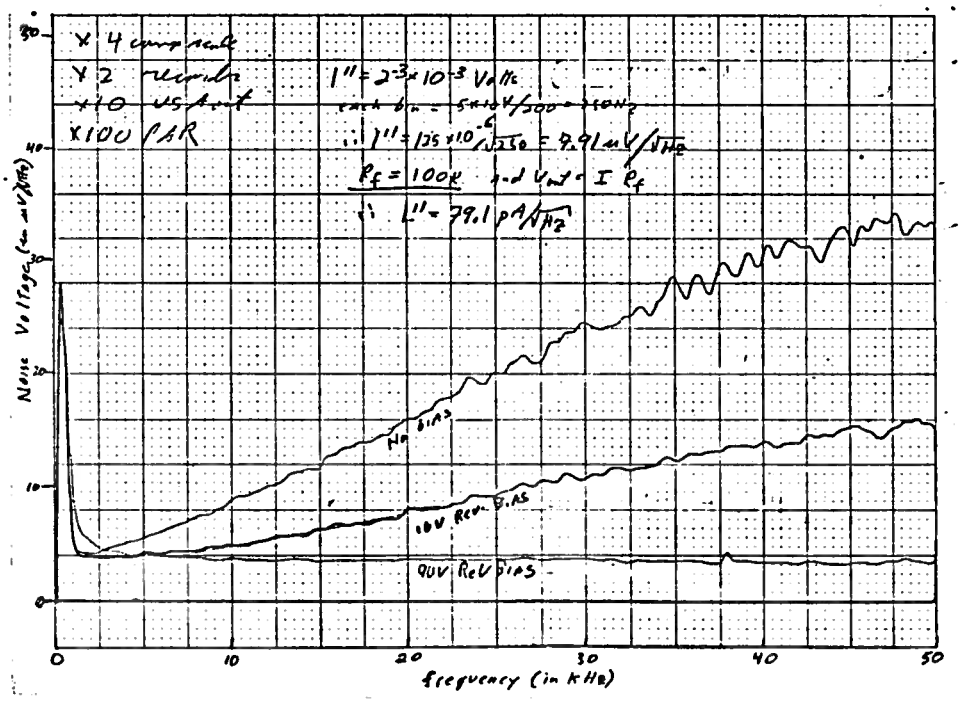

Figure 5.1

Photomultiplier Tube Systems

Because of their built-in current amplifiers, the noise current at the photomultiplier tube cathode may be sufficiently greater than noise currents associated with the op-amp following the tube. Thus in many practical cases, the op-amp will not affect the S/N of the photodetector system. Additionally, photomultiplier tube capacitance (anode to ground) is typically $\sim$ 4 pF, so we are usually free of increased noise due to finite input impedance. For measuring absolute light levels, the S/N of a photodetector system using a photomultiplier tube is

$$S/N = \sqrt{\frac{g-1}{g}} \; \frac{Z_f \; I_{AL}}{\sqrt{\left[\left|1 + \frac{Z_f}{Z_i}\right|^2 e_n^2 + |Z_f|^2 \left(2eGI_{AL} + i_n^2 + \frac{4kT}{R_f} + \frac{4kT}{R_i}\right)\right] \Delta\nu}} \qquad (5.2)$$

The term $2eGI_{AL}$ is the photomultiplier tube shot noise. When the term $|Z_f|^2 \; 2eGI_{AL}\Delta\nu$ dominates in the denominator, we say the system is shot noise, hence photon statistics, limited. For flash photolysis experiments

$$\frac{\delta S}{N} = \sqrt{\frac{g-1}{g}} \; \frac{Z_f \; \delta I_{AL}}{\sqrt{\left\{\left|1 + \frac{Z_f}{Z_i}\right|^2 e_n^2 + |Z_f|^2 \left[2eG(I_{AL}+\delta I_{AL}) + i_n^2 + \frac{4kT}{R_f} + \frac{4kT}{R_i}\right]\right\}\Delta\nu}}$$

or

$$\text{"} = \sqrt{\frac{g-1}{g}} \; \frac{Z_f \; G \Re P_o \; e^{-2.3 \; A_o} \left(e^{-2.3(1-\nu)A_o} - 1\right)}{\sqrt{\left[\left|1 + \frac{Z_f}{Z_i}\right|^2 e_n^2 + |Z_f|^2 \left(2eG^2 \Re P_o \; e^{-2.3(1-\nu)A_o} + i_n^2 + \frac{4kT}{R_f} + \frac{4kT}{R_i}\right)\right] \Delta\nu}} \qquad (5.3)$$

Of interest is the maximum $\delta S/N$, obtained when the system is shot noise limited and ν is optimized. Using Eqs. (3.8) and (5.3), we find

$$\left.\frac{\delta S}{N}\right|_{max} = \sqrt{\frac{g-1}{g}} \quad \sqrt{\frac{\mathcal{R}P_o}{2e\Delta\nu}} \quad 2\eta \left[\frac{(1-\eta)^{1-\eta}}{(1+\eta)^{1+\eta}}\right]^{1/2\eta} \tag{5.4}$$

Photocathode spectral response varies greatly for different photocathode surfaces, but there are many photomultiplier tubes with fairly flat response from 200 nm to 600 nm (variation is within a factor of ~ 2), peaking near 300 nm with quantum efficiencies of $\sim 25\%$, corresponding to responsivities of ~ 0.070 A/W. There are a few photomultiplier tubes whose usable spectral response extends into the near IR.

For illustration, I will examine the $\delta S/N$ in a photodetection system measuring the monitoring beam in a flash photolysis experiment immediately after the actinic flash. I will choose $\eta = 0.9$ (the case for reaction centers), λ (monitoring) = 856 nm, P_o = 100 nW, and $\Delta\nu$ = 1 MHz. For these parameters, the ideal photodetection system, i.e., one whose photomultiplier tube has a Q.E. = 100% $\mathcal{R}(\lambda = 865$ nm), $g >> 1$ and is operating in the shot noise limited regime with A_o (λ = 865 nm) optimized ($A_o = 1.4$), gives a $\delta S/N$ of 265. I will now examine $\delta S/N$ for specific photomultiplier tubes.

The Hammamatsu R955 photomultiplier tube has a $\mathcal{R}(\lambda = 865$ nm) $\simeq 0.0051$ A/W, nine dynode stages with g = 6.0 at v = 100 Volts and a maximum anode current of 10^{-4} A. With all nine dynodes operating the total gain, G, is 1.0×10^7. Immediately after bleaching of the sample the power incident on the photomultiplier tube is P = 100 nW x $10^{-(1-.9)1.42}$ = 72 nW, corresponding to $I_{CL} = 3.7 \times 10^{-10}$ A. In order not to exceed the maximum allowable anode current, seven dynode stages should be used with v = 100 Volts to give $G = 2.8 \times 10^5$. Then $I_{AL} = 1.0 \times 10^{-4}$ A immediately after the actinic flash ($I_{AL} = 5.4 \times 10^{-7}$ A before the flash and $\delta I_{AL} \simeq 1.0 \times 10^{-4}$ A). A suitable amplifier to use for this bandwidth is the OP-16.[17] $C_f \simeq 5$pF from stray capacitance, $R_f = 10^4\ \Omega$ to insure maximum conversion gain within the chosen bandwidth, $C_i \simeq 4$pF for this tube, and R_i is essentially infinite.

[17]Manufactured by the Precision Monolithics Corporation.

Using Eq. (5.3), integrating the noise over frequency, we find $\delta S/N \simeq 31$. This is the shot noise limited result as checked by comparing terms in the denominator of Eq. (5.3).

The Hammamatsu R666S photomultiplier tube has a $\mathcal{R}(\lambda = 865\ nm) = 0.0167$ A/W, nine dynode stages with g = 4.7 at v = 100 Volts and a maximum anode current of 10^{-5} A. With all nine dynodes operating, $G = 1.2 \times 10^{6}$. Immediately after bleaching of the sample, $I_{CL} = 1.2 \times 10^{-9}$ A. In order not to exceed the maximum allowable anode current, six dynode stages should be used with v = 94 Volts (g = 4.50) to give $G = 8.3 \times 10^{3}$. Then $I_{AL} = 1.0 \times 10^{-5}$ A immediately after the actinic flash. Using the OP-16 amplifier, as in the previous example, Eq. (5.3) predicts $\delta S/N = 54$. Again, this is the shot noise limited value.

The RCA C31034 is the most sensitive photomultiplier tube available with an essentially flat spectral response from 280 nm to 860 nm. It has a $\mathcal{R}(\lambda = 865\ nm) = .110$ A/W, 11 dynode stages with g = 3.4 at v = 125 Volts and a maximum anode current of 10^{-7} A. It is recommended that the tube be used at reduced temperatures. Clearly this photomultiplier tube is best suited for low-light ($P < 10^{-6}$ W) detection. Immediately after bleaching of the sample, $I_{CL} = 7.9 \times 10^{-9}$ A. In order not to exceed the maximum allowable anode current, two dynode stages should be used with v = 135 Volts (g = 3.6) to give G = 13. Then $I_{AL} = 1.0 \times 10^{-7}$ A immediately after the actinic flash. In conjunction with the OP-16 amplifier, Eq. (5.3) predicts $\delta S/N = 41$. This is about three times lower than the shot noise limited value of $\delta S/N = 132$. Due to the small anode current, the photodetector system noise is now limited by Johnson noise in the op-amp feedback resistor and the e_n of the OP-16. This photomultiplier tube can be used in a shot noise limited photosystem when $I_{AL} \approx 10^{-7}$ A for $e_n \lesssim 5\ nV/\sqrt{Hz}$, obtainable with a low noise FET front ended op-amp, and $R_f \gtrsim 10^{5}\ \Omega$. These changes will limit the bandwidth of the system to $\sim 10^{5}$ Hz.

If one chooses to use the previously described photodetection system for msec rather than μsec time resolution, a bandwidth of 1 KHz will allow all three

photomultiplier tube detection systems to operate in the shot noise limited region. $\delta S/N$ will then be 980, 1700, and 4200 for the R955, R666S, and C31034 photomultiplier tube photodetection systems, respectively.

Photodiode Systems

Photodiodes do not contain any internal amplification and their use with op-amps will in general degrade the photosystem S/N. In addition, photodiode junction capacitance is high, $\sim$ 500 pF/(cm^2 detection area), so there may be enhancement of noise at high frequencies. To alleviate this last problem, the junction capacitance can be decreased by applying a reverse bias potential to the photodiode. This bias has the effect of increasing the width of the depletion region in the photodiode, therefore, decreasing the junction capacitance. The relationship between this capacitance and bias potential is given by[18]

$$C_p = \frac{C_{po}}{(1-V/V_o)^{1/2}}$$

where C_{po} is the photodiode junction capacitance at zero bias and V_o is a constant dependent on the properties of the photodiode. The application of a reverse bias potential contributes an additional shot noise component due to the reverse bias current I_B. For measuring absolute light levels, the S/N for a photodiode detector system is:

$$\frac{S}{N} = \frac{Z_f I_L}{\sqrt{\left[\left|1 + \frac{Z_f}{Z_p}\right|^2 e_n^2 + |Z_f|^2 \left(2eI_L + 2eI_B + i_n^2 + \frac{4kT}{R_f} + \frac{4kT}{R_p(0)}\right)\right] \Delta\nu + I_{EX}^2}} \quad \ldots(5.5)$$

[18] "Heterojunctions and Metal-Semiconductor Junction" - Milnes and Feucht, Chapter 2.

For flash photolysis experiments

$$\frac{\delta S}{N} = \frac{Z_f \, \delta I_L}{\sqrt{\left\{\left|1 + \frac{Z_f}{Z_p}\right|^2 e_n^2 + |Z_f|^2 \left[2e(I_L+\delta I_L)+2eI_B+i_n^2 + \frac{4kT}{R_f} + \frac{4kT}{R_p(0)}\right]\right\}\Delta\nu + I_{EX}^2}}$$

or

$$" = \frac{Z_f \mathcal{R} P_o \, e^{-2.3A_o} \, (e^{2.3\nu A_o} - 1)}{\sqrt{\left[\left|1 + \frac{Z_f}{Z_p}\right|^2 e_n^2 + |Z_f|^2 \left(2e \mathcal{R} P_o \, e^{-2.3(1-\nu)A_o} + 2eI_B + i_n^2 \quad \ldots \right.\right.}}$$

$$\left.\left. \ldots + \frac{4kT}{R_f} + \frac{4kT}{R_p(0)}\right)\right] \Delta\nu + I_{EX}^2}$$

(5.6)

In Eq. (5.6), I_{EX} must be evaluated at $I_L + \delta I_L$. The decision as to when to apply a reverse bias depends simply upon whether or not the S/N or δS/N is increased or decreased, which must come from direct evaluation of Eq. (5.5) or Eq. (5.6) under the two conditions. As a general and obvious rule of thumb, when constructing a photodetection system to work at high frequencies, reverse bias is preferable, when working at low frequencies, it may only add noise to the system. Using as an example the flash photolysis experiment described in conjunction with photomultiplier tube detection systems, I will consider two examples.

For a bandwidth of 1 MHz, the op-amp (OP-16) input voltage noise, e_n, and the Johnson noise of the feedback resistor (R_f = 10 KΩ) will dominate if I_L, $I_B \ll 5 \times 10^{-6}$ A. I will neglect I_{EX} under the assumption that data is collected

for a few msec at most, giving a low frequency cutoff of ∿ 1 KHz. Most photodiodes of interest have $\mathcal{R}(\lambda = 865\ ) = .4$ and $R_d(0)$ sufficiently large as to be taken as infinite is S/N calculations. With these parameters, Table 5.1 was constructed using Eq. (5.6) to illustrate the effect of C_p on the δS/N.

C_p	δS/N
0	15
5 pF	14
10 pF	13
20 pF	10
50 pF	5.4

Table 5.1

The lowest capacitance photodiode available is the UDT-020A with C_p = 1.9 pF at V_{bias} = -50 Volts. This diode has $\mathcal{R}(\lambda = 865\ nm) = .4$, $R_d = 10^{11}\ \Omega$, $I_B = 7.5 \times 10^{-11}$ A and a photosensitive area of .002 cm^2. The δS/N is calculated to be 14.5. In practice, the op-amp input capacitance, C_i, may be greater than C_p by a few pF due to finite lead length. Also, the photosensitive area is extremely small. A more reasonable choice of photodiodes for a laboratory detection system is the UDT-5D. This diode has C_p = 6 pF at V_{bias} = -50 Volts, $\mathcal{R}(\lambda = 865\ nm) = .4$, $R_d \approx 10^9\ \Omega$, $I_B = 2 \times 10^{-8}$ A and a photosensitive area of .050 cm^2. The δS/N is calculated to be 13.2.

For a bandwidth of 1 KHz, photodiode junction capacitance is no longer as important. Also, the lower bandwidth will allow a larger R_f (R_f = 10 MΩ). I will choose as a photodiode the UDT-6D, whose excess noise characteristics have been discussed in Section II. This photodiode has C_p = 120 pF at V_{bias} = 0, $R_d = 9 \times 10^7\ \Omega$, $\mathcal{R}(\lambda = 865\ nm) = .4$ and a photosensitive area of .203 cm . The total excess noise is found by integrated $I_{EX} = 5 \times 10^{-4}\ I_L/f^{4/5}$ from f = 1 to f = 1000 Hz (this assumes a 1 sec data collection period), where the form of I_{EX}

was taken from Figure 2.8. We find $\delta S/N = 115$, essentially limited by the excess noise. Op-amp noise sources will only dominate after a 10^2-10^3 reduction in optical power. Photodetector systems using photodiodes whose excess noise flattens out at low frequencies will have a somewhat better $\delta S/N$.

Concluding Remarks

It has been shown that photomultiplier tubes are superior to photodiodes for use in photodetection systems measuring the monitoring beam in flash photolysis. This holds for both high (MHz) and low (KHz) frequency systems. Photodiodes should only be considered with the $\delta S/N$ is sufficiently high that the extra cost and space of a photomultiplier tube makes the photodiode acceptable. The $\delta S/N$ of a photomultiplier tube detection system can be improved by increasing the monitoring beam intensity so that $(I_{AL} + \delta I_{AL})$ is greater than the maximum allowed value for short periods of time. Only the average of I_{AL} over some time limit, usually 30 sec, must be below a maximum value. RCA reports that it has pulsed photomultiplier tubes to 1000 times their average maximum I_{AL} without damage. As P_o is increased to increase the $\delta S/N$, the sample may begin to bleach due to the monitoring beam intensity. Since the amount of bleaching is proportional to the time the monitoring beam is on, one can turn the monitoring beam on just before the actinic flash to reduce this artifact from the measuring process. This technique is known as pulsing the monitoring beam, and applies to photodiode as well as photomultiplier tube photodetection systems.

List of Major Symbols Used

A	Optical absorbance of sample
C_f	Feedback capacitance
C_i	Input capacitance
C_p	Photodiode junction (parallel) capacitance
e	Electronic charge
e_n	Op-amp input noise voltage per root hertz
E_n	Output noise voltage
Eg	Band gap energy of PIN photodiode
E_{WF}	Work function of photomultiplier tube cathode surface
f	Circular frequency
g	Current gain of individual dynode stage in photomultiplier tube
G	Total current gain of photomultiplier tube
i_n	Op-amp input noise current per root hertz
I_{AD}	Anode dark current in photomultiplier tubes
I_{AL}	Light-induced anode current in photomultiplier tubes
I_B	Photodiode bias current
I_{CD}	Cathode dark current in photomultiplier tubes
I_{CL}	Light-induced cathode current in photomultiplier tubes
I_{EX}	Excess noise current
I_i	Input current
I_{IN}	Component of current noise independent of I_L
I_L	Light-induced current in photodiodes
I_N	Noise current
I_S	Photodiode reverse bias saturation current
I_{SH}	Photodetector shot noise
k	Boltzmann's constant
P	Power incident or photodetector

(Continued next page)

P_o	Power incident on sample
Q.E.	Photodetector quantum efficienty
R_f	Feedback resistance
R_i	Input resistance
R_p	Photodiode junction (parallel) resistance
R_s	Photodiode series resistance
$\mathcal{R}(\lambda)$	Photodetector responsivity
S/N	Signal-to-noise ratio for measuring absolute light levels
δS/N	Signal-to-noise ratio for measuring changes in a light level
T	Temperature
v	Voltage drop across photomultiplier tube dynode stage
V	Voltage drop across photomultiplier tube (high voltage supply)
V_L	Light-induced voltage
V_i	Input voltage
Z_d	Photodiode impedance
Z_f	Feedback impedance
Z_i	Input impedance
Z_p	Photodiode junction (parallel) impedance
$\alpha(f)$	Photodiode excess noise frequency distribution function
$\delta\chi$	Variation, or change, in χ
$\mathcal{Y}$	Fractional optical bleaching of sample
λ	Wavelength
ν	Circular frequency
ω	Radian frequency

Acknowledgements

This problem was originally suggested by Tim Marinetti. George Feher offered guidance and stimulating discussion during this project. Discussions with Don Fredkin were most useful, especially in understanding the physics of PIN photodiodes. Mel Okamura and Shelly Schultz offered lucid comments on my results. Mel also first brought up the idea of partition noise. Roger Isaacson offered his usual sage advice in making the experimental measurements, and in building the new photodetector system.